Towards a consistent approach for nuclear structure and reactions: microscopic optical potentials,
ECT, Trento, June 17 – 21, 2024*

Relativistic ab initio description of nucleon-nucleus elastic scattering in the full Dirac space

Sibo Wang （王锶博）

Department of Physics, Chongqing University, China *sbwang@cqu.edu.cn*

P. Qin, S. Wang*, H. Tong, Q. Zhao, C. Wang, Z.P. Li, and P. Ring, Phys. Rev. C **109**, 064603 (2024), **Editor's Suggestion**

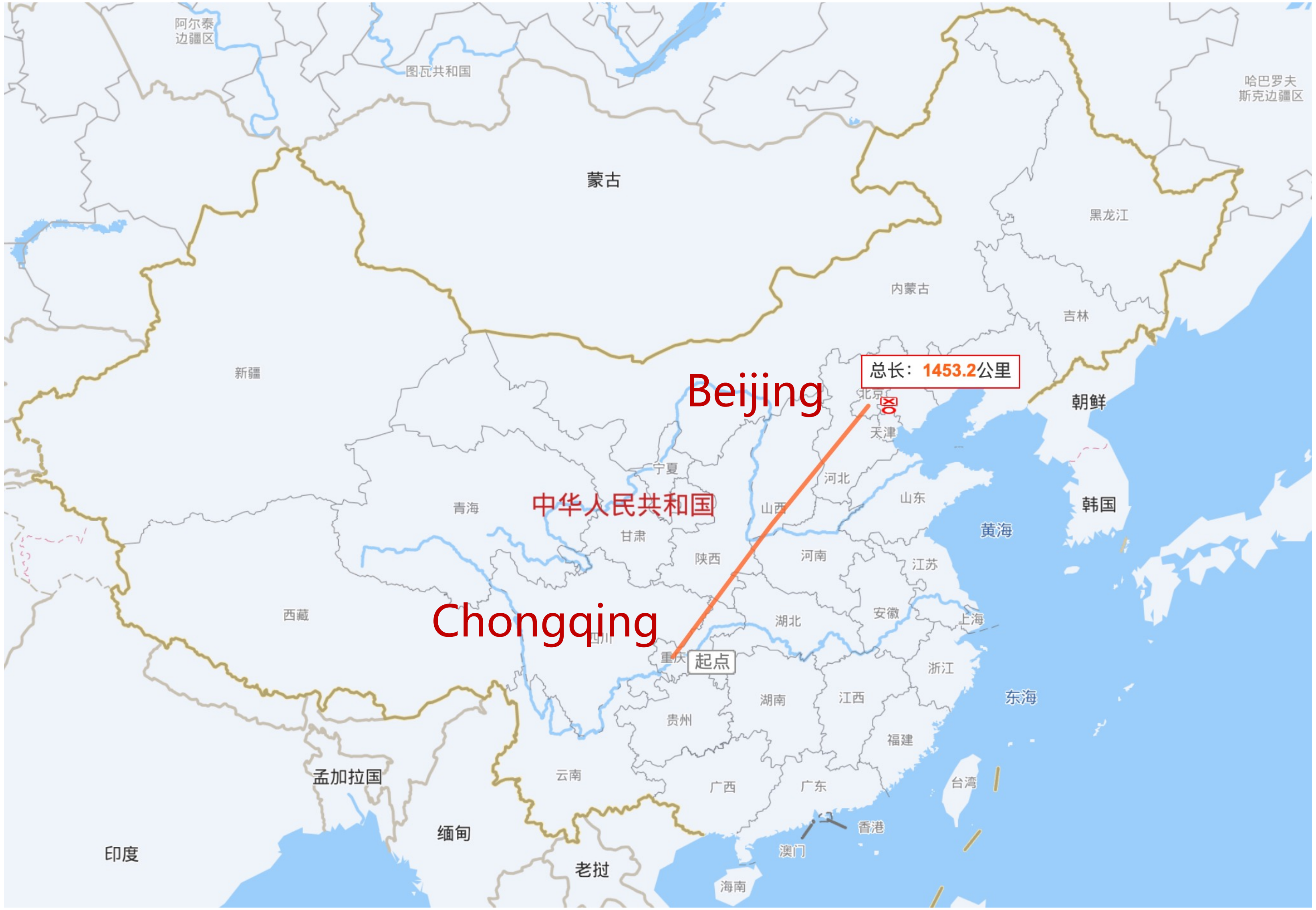
Beijing
Chongqing
中华人民共和国
总长：1453.2公里
起点
北京
天津
重庆
四川
河北
山西
山东
河南
陕西
甘肃
宁夏
青海
新疆
西藏
内蒙古
吉林
黑龙江
湖北
安徽
江苏
上海
浙江
湖南
江西
福建
贵州
云南
广西
广东
香港
澳门
海南
台湾
蒙古
朝鲜
韩国
黄海
东海
孟加拉国
缅甸
印度
老挝
图瓦共和国
阿尔泰
边疆区
哈巴罗夫
斯克边疆区

Contents

Nucleon-nucleus scattering

- Nuclear reaction——An important branch of nuclear physics
  - ✓ Revealing NN interactions, structural and dynamic properties of nuclei
  - ✓ Understanding the evolution of the stars and the origin of the elements
  - ✓ Applications on medical therapy, nuclear power, national security, etc.

- Nucleon-nucleus scattering——One of the simplest processes of nuclear reaction
  - ✓ Exact solution of the $A + 1$ many-body problem is hard to achieve

  → **optical model**: complex mean field (optical potential)

$$U(r,E) = V(r,E) + iW(r,E)$$

Elastic scattering   Inelastic channels

Phenomenological optical potential

- Nonrelativistic: volume, surface, and spin-orbit terms
  - ✓ KD03: $1\ \mathrm{keV} \le E \le 200\ \mathrm{MeV}, 24 \le A \le 209$ Koning and Delaroche, NPA **713**, 231 (2003)
- Relativistic: spin-orbit terms are naturally included
  - ✓ GOP: $20 \le E \le 1040\ \mathrm{MeV}, 4 \le A \le 208$ Hama, Clark, Cooper *et al.*, PRC (1990, 1993, 2006, 2009)

Large extrapolations for KD03 are inevitable.

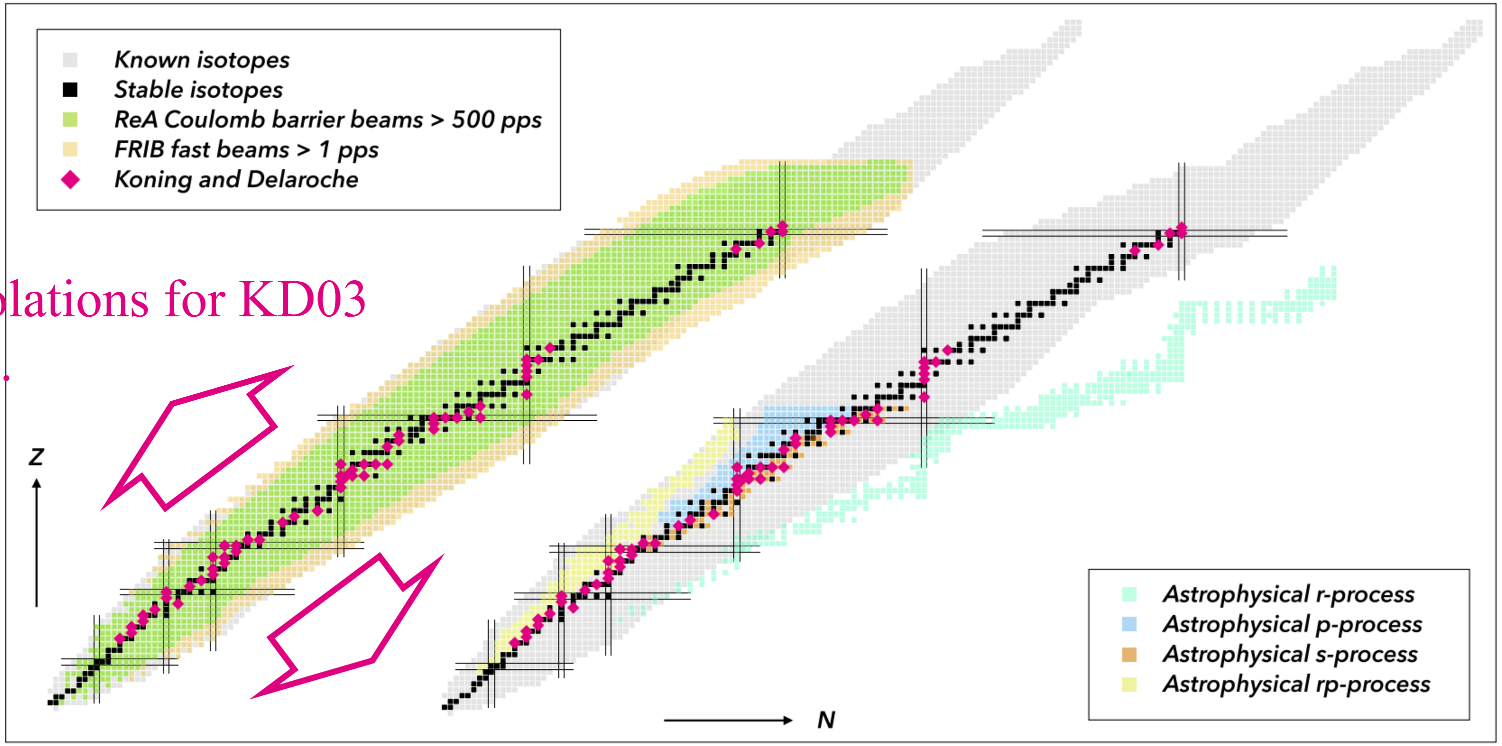

Microscopic optical potential

- Folding method: NN scattering amplitudes folded with densities of the target

Watson, Phys. Rev. **89**, 575 (1953), Kerman, McManus, and Thaler, Ann. Phys. **8**, 551 (1959)

$$U(r,\varepsilon) = \int V(\boldsymbol{r},\boldsymbol{r}',\varepsilon)\cdot\rho(\boldsymbol{r}')\, d\boldsymbol{r}'$$

  - T matrix folding: Elster, Cheon, Redish, and Tandy, Phys. Rev. C **41**, 814 (1990)
  - G matrix folding: Furumoto, Sakuragi, and Yamamoto, Phys. Rev. C **78**, 044610 (2008)

- Local density approximation (LDA): optical potentials equivalent to single-particle potentials in nuclear matter Bell and Squires, PRL **3**, 96 (1959), Jeukenne, Lejeune, and Mahaux. PRC **16**, 80 (1977)

$$U_{\mathrm{LDA}}(r,\varepsilon) = U_{\mathrm{NM}}(\varepsilon,\rho(r),\alpha(r))$$

  - Brueckner-Hartree-Fock (BHF): Bauge, Delaroche, and Girod, Phys. Rev. C **58**, 1118 (1998)
  - Many-body perturbation theory: Whitehead, Lim, and Holt, Phys. Rev. Lett. **127**, 182502 (2021)
  - Relativistic BHF (RBHF): R. Xu, *et al.*, Phys. Rev. C **94**, 034606 (2016), G.Q. Li and Y.Z. Zhuo, Nucl. Phys. A **568**, 745 (1994)

Relativistic microscopic optical potential — — CTOM

- CTOM: *Optical Model by co-operation between China Nuclear Data Center & Tuebingen University*
  - $E \leq 200$ MeV, $^{12}C - {}^{208}Pb$
  - Minor adjustments in the low-density region
  - (Improved) LDA+RBHF (negative-energy states neglected) R. Xu, *et al.* PRC **94**, 034606 (2016)

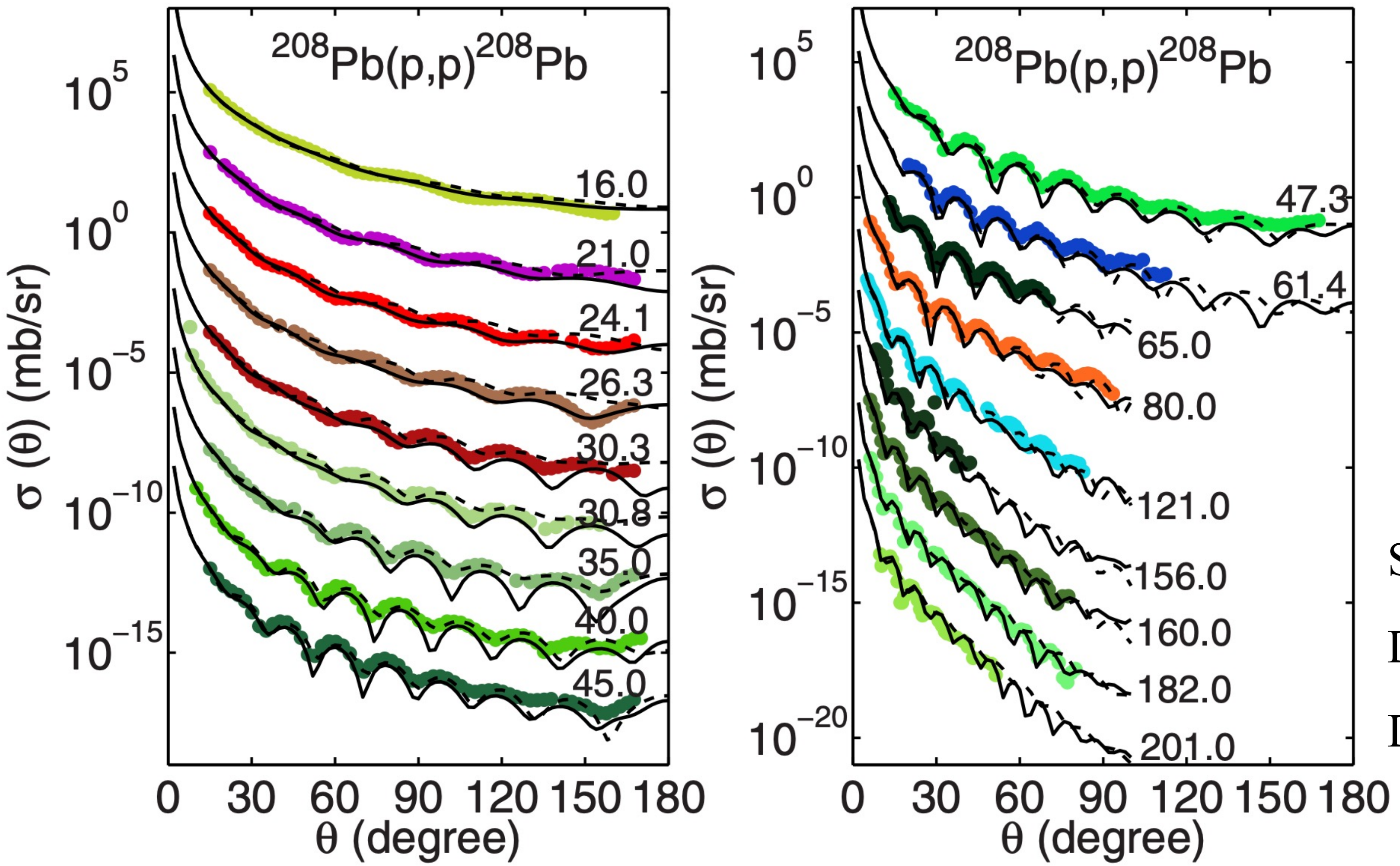

Solid: CTOM

Dashed: KD03

Dots: Exp.

Importance of the negative-energy states

- Negative-energy states (NESs) are indispensable for the completeness of a basis.

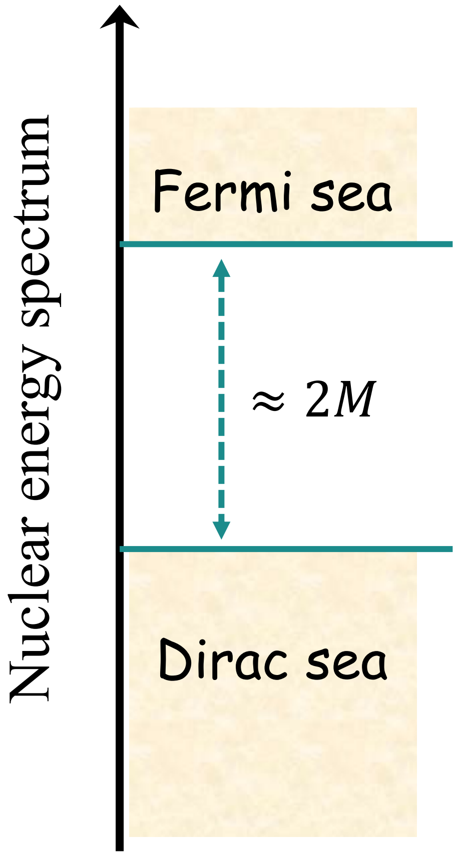

$$\psi_{\alpha\kappa m}(\boldsymbol{r}) = \sum_n c_{\alpha n}\psi^{0+}_{n\kappa m}(\boldsymbol{r}) + \sum_{n'} d_{\alpha n'}\psi^{0-}_{n'\kappa m}(\boldsymbol{r})$$

7% less binding for ^{16}O is found without NESs.

Zhou, Meng, and Ring, Phys. Rev. C **68**, 034323 (2003)

$$u(\boldsymbol{p},\lambda) = a_+ u_0(\boldsymbol{p},\lambda) + a_- v_0(\boldsymbol{p},\lambda)$$

Insufficient repulsion for nuclear matter is found without NESs.

Anastasio, Celenza, and Shakin, Phys. Rev. C **23**, 2273 (1981)

Attention: considering NESs dose NOT mean to avoid the *no-sea approximation*.

RBHF theory in the full Dirac space

- Self-consistent solution of RBHF theory in the full Dirac space has been achieved for nuclear matter

Wang, Zhao, Ring, and Meng, PRC **103**, 054319, PRC **106**, L021305

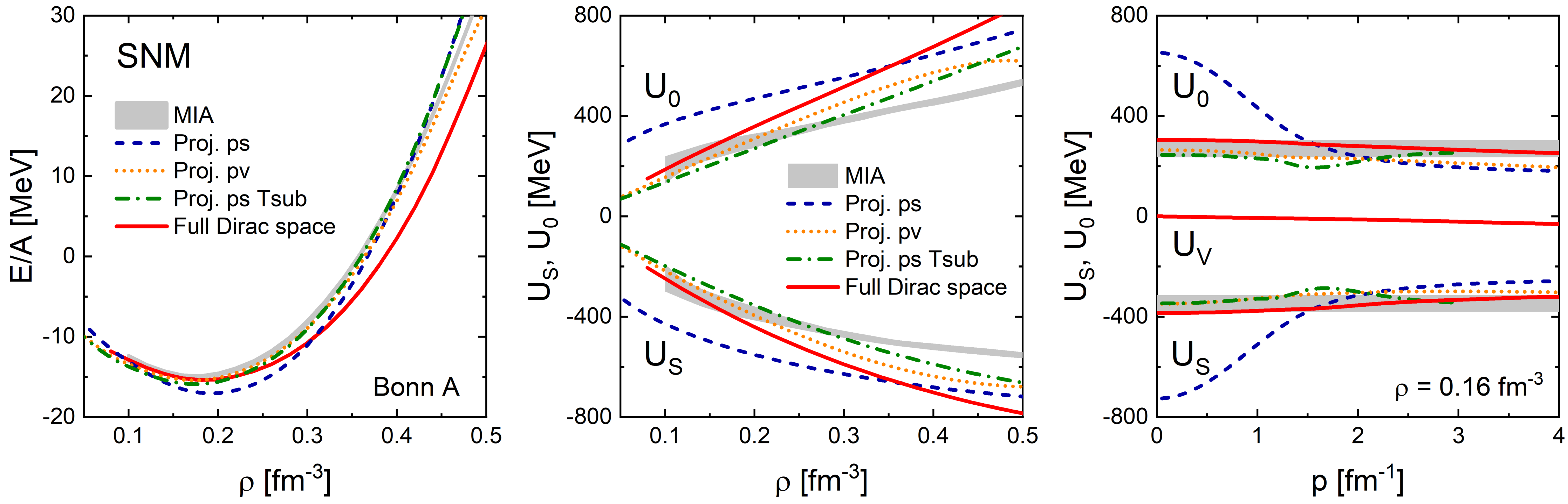

To describe nucleon-nucleus scattering with RBHF theory in the full Dirac space

Contents

Bonn potential

- Our starting point of ab initio: the *one-boson-exchange* model   R. Machleidt, ANP **19**, 189 (1989)

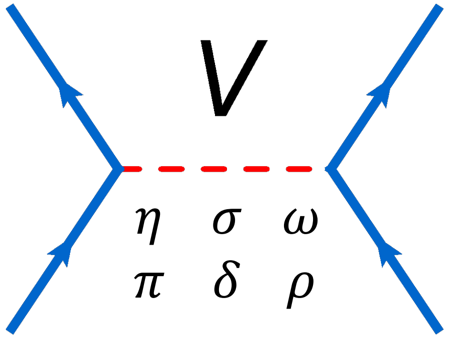

$$\mathcal{L}_s = +g_s \bar{\psi}\psi\varphi^{(s)},$$

$$\mathcal{L}_{ps} = -\frac{f_{ps}}{m_{ps}} \bar{\psi}\gamma^5\gamma^\mu\psi\partial_\mu\varphi^{(ps)},$$

$$\mathcal{L}_v = -g_v\bar{\psi}\gamma^\mu\psi\varphi_\mu^{(v)} - \frac{f_v}{4M}\bar{\psi}\sigma^{\mu\nu}\psi(\partial_\mu\varphi_\nu^{(v)} - \partial_\nu\varphi_\mu^{(v)}).$$

→ *most economical and quantitative phenomenology for describing the NN interaction*

R. Machleidt and D.R. Entem, Phys. Rep. **503**, 1 (2011)

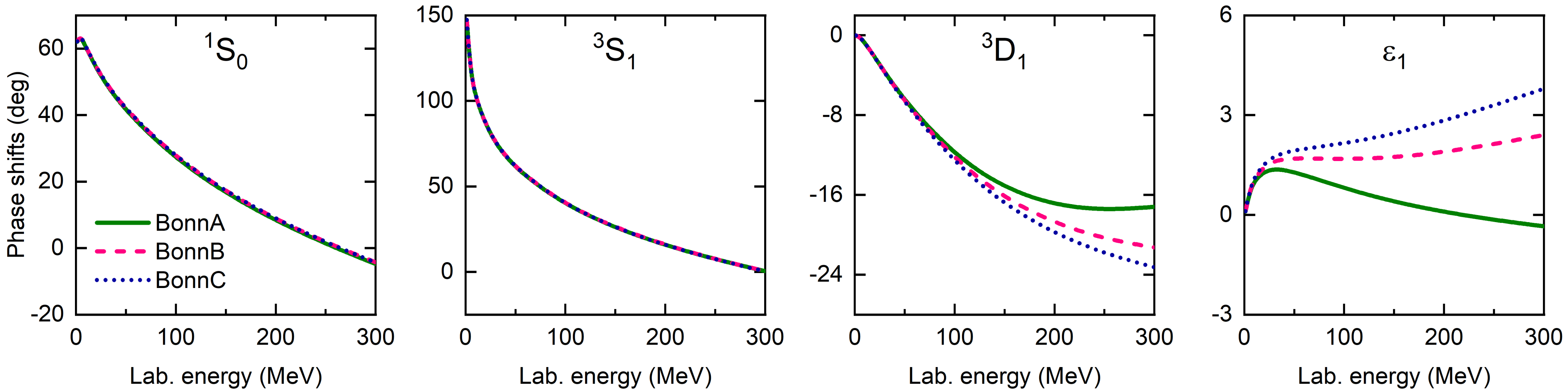

Dirac equation in nuclear matter

$$\{\boldsymbol{\alpha}\cdot\boldsymbol{p}+\beta[M+\mathcal{U}(\boldsymbol{p})]\}\,u(\boldsymbol{p},s)=E_p u(\boldsymbol{p},s)$$

Single-particle potential $\mathcal{U}(\boldsymbol{p})=U_S(p)+\gamma^0 U_0(p)+\boldsymbol{\gamma}\cdot\hat{\boldsymbol{p}}U_V(p)$

scalar timelike spacelike

$$[\boldsymbol{\alpha}\cdot\boldsymbol{p}^*+\beta M_p^*]u(\boldsymbol{p},s)=E_p^* u(\boldsymbol{p},s)$$

Effective quantities $M_p^*=M+U_S,\quad \boldsymbol{p}^*=\boldsymbol{p}+\hat{\boldsymbol{p}}U_V(p),\quad E_p^*=E_p-U_0(p)$

Positive-energy $u(\boldsymbol{p},s)=\sqrt{(E_p^*+M_p^*)/2M_p^*}\,[1,\boldsymbol{\sigma}\cdot\boldsymbol{p}^*/(E_p^*+M_p^*)]^T\chi_s$

Negative-energy $v(\boldsymbol{p},s)=\gamma^5 u(\boldsymbol{p},s)$

$$\sum_{\boldsymbol{s}} u(\boldsymbol{p},s)\,\bar{u}(\boldsymbol{p},s)-v(\boldsymbol{p},s)\,\bar{v}(\boldsymbol{p},s)=\mathbf{1}_{4\times4}$$

Extract the single-particle potentials

- Nucleon-nucleon scattering equation in the nuclear medium

$$\begin{bmatrix} G^{++++} \\ G^{-+++} \end{bmatrix}(\boldsymbol{q}',\boldsymbol{q}|\boldsymbol{P},W) = \begin{bmatrix} V^{++++} \\ V^{-+++} \end{bmatrix}(\boldsymbol{q}',\boldsymbol{q}|\boldsymbol{P})$$

$$+\int \frac{d^3k}{(2\pi)^3}\begin{bmatrix} V^{++++},0 \\ V^{-+++},0 \end{bmatrix}(\boldsymbol{q}',\boldsymbol{k}|\boldsymbol{P})\frac{Q(\boldsymbol{k},\boldsymbol{P})}{W-E_{\boldsymbol{P}+\boldsymbol{k}}-E_{\boldsymbol{P}-\boldsymbol{k}}}\begin{bmatrix} G^{++++} \\ G^{-+++} \end{bmatrix}(\boldsymbol{k},\boldsymbol{q}|\boldsymbol{P},W)$$

- Matrix elements of the single-particle potential operator

$$\Sigma^{hh'}(p) = \langle \bar{h}|\mathcal{U}(\boldsymbol{p})|h'\rangle = \int \frac{d^3p'}{(2\pi)^3}\frac{M^*_{p'}}{E^*_{p'}}\bar{G}^{h+h'+}(\boldsymbol{q},\boldsymbol{q}|\boldsymbol{P},W), \qquad h,h' = +,-$$

- Scalar and vector components of single-particle potential

$$U_S(p) = \frac{\Sigma^{++}(p)-\Sigma^{--}(p)}{2}$$

$$U_0(p) = \frac{E^*_p}{M^*_p}\frac{\Sigma^{++}(p)+\Sigma^{--}(p)}{2} - \frac{p^*}{M^*_p}\Sigma^{-+}(p)$$

$$U_V(p) = -\frac{p^*}{M^*_p}\frac{\Sigma^{++}(p)+\Sigma^{--}(p)}{2} + \frac{E^*_p}{M^*_p}\Sigma^{-+}(p)$$

⇨ *No ambiguities!*

Self-consistent treatment for the imaginary parts

- Thompson equation within the *continuous choice* for particle and hole states

$$
\begin{aligned}
&\langle q'|G^J(P,W)|q\rangle \\
&= \langle q'|V^J|q\rangle + \int \frac{k^2 dk}{(2\pi)^3}\langle q'|V^J|k\rangle \frac{Q_{\rm av}(k,P)}{W-2E_{\rm av}(k,P)}\langle k|G^J(P,W)|q\rangle - \langle q'|V^J|k_0\rangle \\
&\quad \times Q_{\rm av}(k_0,P)\frac{W+2E_{\rm av}(k_0,P)}{A(k_0,P)}\left[k_0^2\int\frac{dk}{(2\pi)^3}\frac{1}{4(k_0^2-k^2)}+\frac{i\pi}{(2\pi)^3}\frac{k_0}{8}\right]\langle k_0|G^J(P,W)|q\rangle .
\end{aligned}
$$

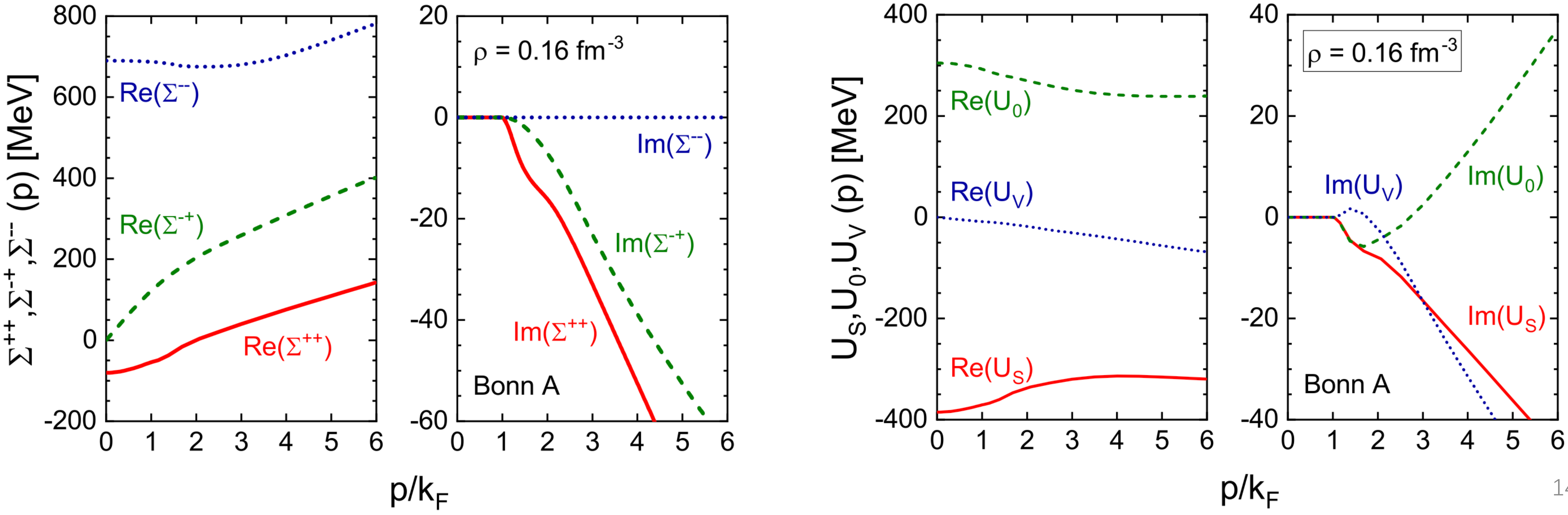

Application: Isospin splitting of Dirac mass

$$M^*_{D,\tau} = M + U_{S,\tau}, \qquad \tau = n, p$$

- Full Dirac space

  $M^*_{D,n} < M^*_{D,p}$

- Projection

  $M^*_{D,n} < M^*_{D,p}$

- Mom.-ind. app.

  $M^*_{D,n} > M^*_{D,p}$

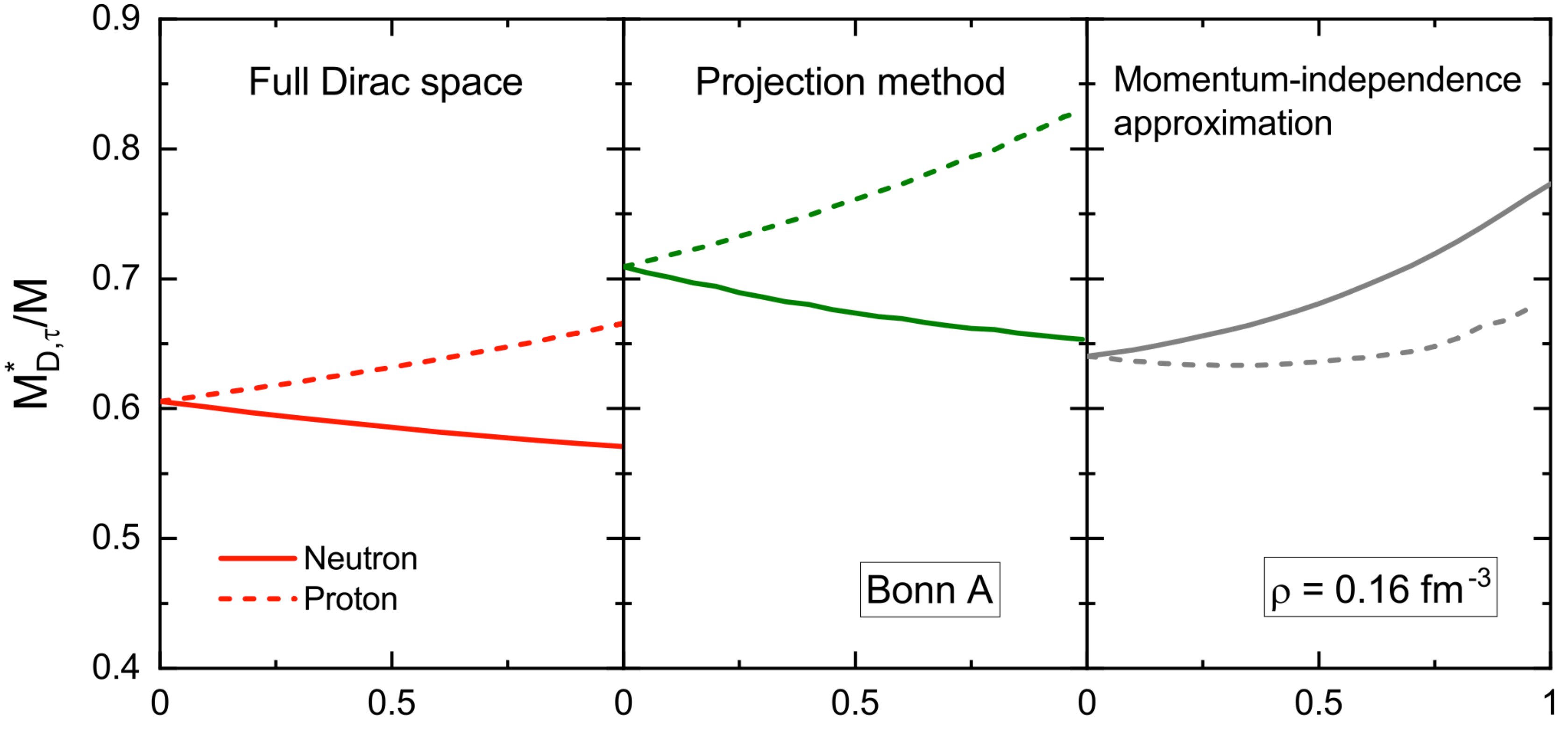

$$\alpha = (\rho_n - \rho_p)/\rho$$

The long standing controversy is clarified. Wang, Tong, Zhao, Wang, Ring, and Meng, PRC **106**, L021305 (2022)

Application: Isospin splitting of nonrelativistic effective mass

$$\frac{M^*_{NR,\tau}}{M} = \left[1 + \frac{M}{p}\frac{dU_{\mathrm{S.e.}}}{dp}\Big|_{p=k_F^\tau}\right]^{-1}, \qquad U_{\mathrm{S.e.}} = (U_S^2 - U_0^2 + 2EU_0 + 2MU_S)/2M$$

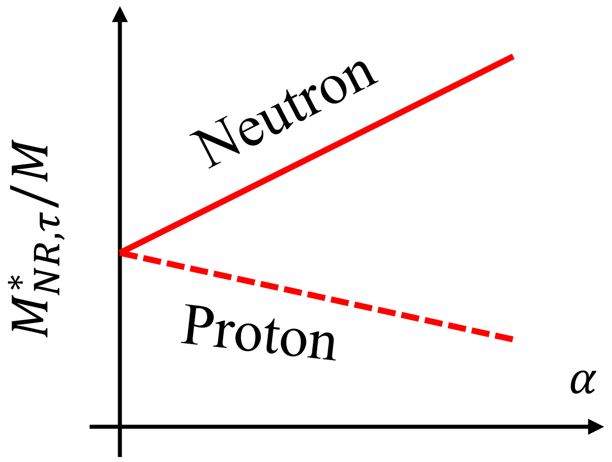

$(M_{NR,n} - M_{NR,p})/(M\alpha) = \text{const.}$

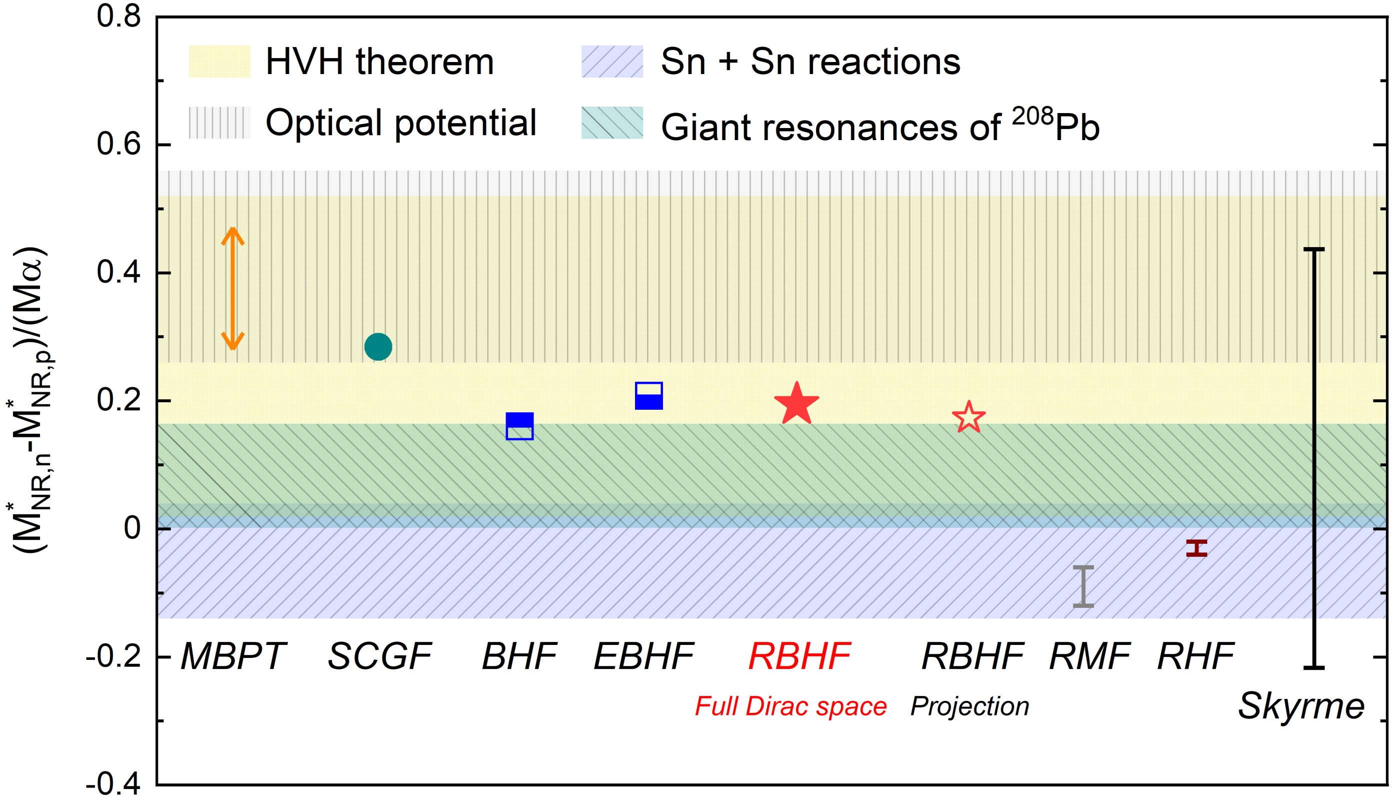

$\rightarrow (M^*_{NR,n} - M^*_{NR,p})/(M\alpha) = 0.187$

Wang, Tong, Zhao, Wang, Ring, and Meng, PRC **108**, L031303 (2023)

Application: Neutron star structural properties

- Mass, radius, and tidal deformability of neutron stars in the full Dirac space

$R_{1.4\odot} = 11.97$ km, $M_{max} = 2.43\ M_{\odot}$, $\Lambda_{1.4\odot} = 376$

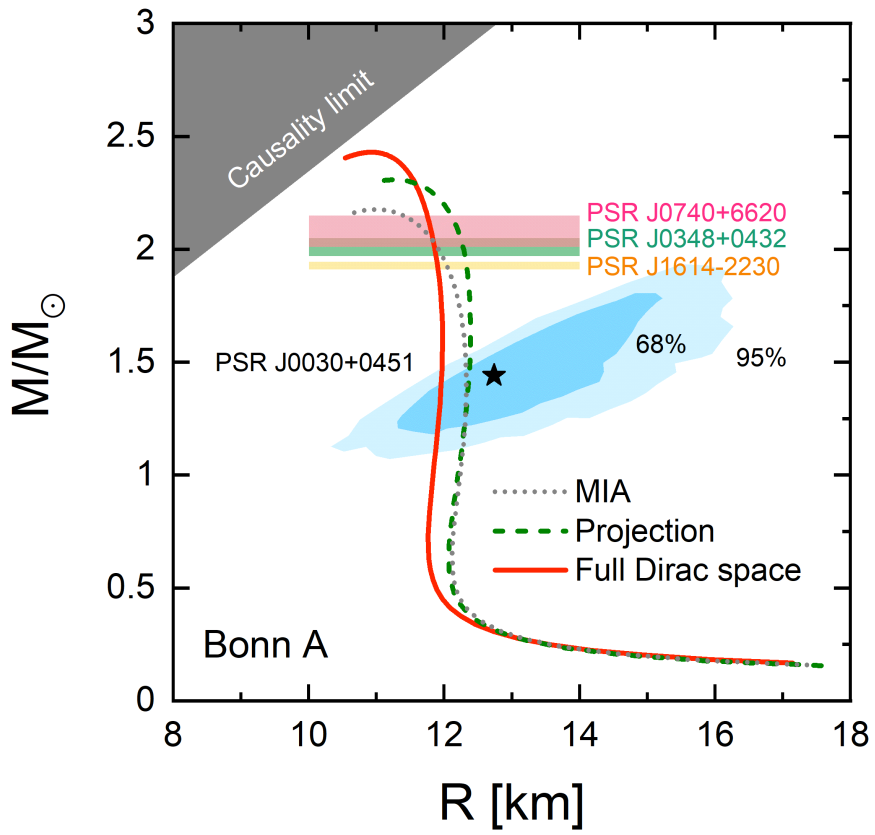

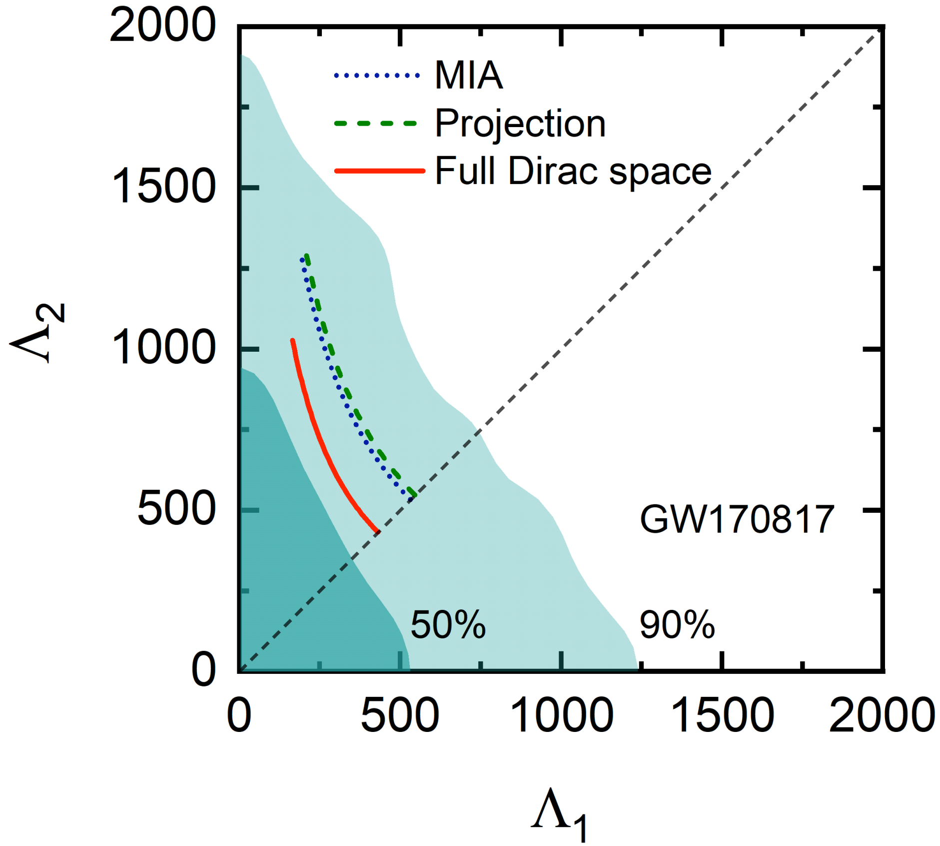

Tong, Wang, and Wang, ApJ **930**, 137 (2022)

Qu, Tong, Wang, and Wang, Sci. China-Phys. Mech. Astron. **66**, 242011 (2023)

Local density approximation

- LDA: Optical potential at distance r is locally related to nuclear matter

$$U_{\mathrm{LDA}}(r,\varepsilon)=U_{\mathrm{NM}}(\varepsilon,\rho(r),\alpha(r))$$

$$\rho=\rho_n+\rho_p$$
$$\alpha=(\rho_n-\rho_p)/\rho$$

- Improved LDA (ILDA): consider finite range correction of nuclear forces

$$U_{\mathrm{ILDA}}(r,\varepsilon)=(t\sqrt{\pi})^{-3}\int U_{\mathrm{LDA}}(r',\varepsilon)\exp[-(\boldsymbol{r}-\boldsymbol{r}')^2/t^2]d^3r'$$

- ✓ JLMB: $t_{p-\mathrm{A}}=1.2$ fm, $t_{n-\mathrm{A}}=1.3$ fm E. Bauge *et al.*, PRC **58**, 1118 (1998)
- ✓ CTOM: $t_{p-A}=1.25$ fm, $t_{n-A}=1.35$ fm R. Xu *et al.*, PRC **94**, 034606 (2016)
- ✓ WLH: $t_{\mathrm{cent}}=1.22$ fm, $t_{\mathrm{so}}=0.98$ fm T.R. Whitehead *et al.*, PRL **127**, 182502 (2021)

In this work $t=1.3$ fm is adopted by default. Uncertainties are shown later.

Density profile: RMF theory with PC-PK1

Point-coupling Lagrangian density:

$$
\begin{aligned}
\mathcal{L} = {} & \bar{\psi}(i\gamma_\mu\partial^\mu - m)\psi \\
& -\frac{1}{2}\alpha_S(\bar{\psi}\psi)(\bar{\psi}\psi) - \frac{1}{2}\alpha_V(\bar{\psi}\gamma_\mu\psi)(\bar{\psi}\gamma^\mu\psi) \\
& -\frac{1}{2}\alpha_{TS}(\bar{\psi}\vec{\tau}\psi)(\bar{\psi}\vec{\tau}\psi) - \frac{1}{2}\alpha_{TV}(\bar{\psi}\vec{\tau}\gamma_\mu\psi)(\bar{\psi}\vec{\tau}\gamma^\mu\psi) \\
& -\frac{1}{3}\beta_S(\bar{\psi}\psi)^3 - \frac{1}{4}\gamma_S(\bar{\psi}\psi)^4 - \frac{1}{4}\gamma_V\left[(\bar{\psi}\gamma_\mu\psi)(\bar{\psi}\gamma^\mu\psi)\right]^2 \\
& -\frac{1}{2}\delta_S\partial_\nu(\bar{\psi}\psi)\partial^\mu(\bar{\psi}\psi) - \frac{1}{2}\delta_V\partial_\nu(\bar{\psi}\gamma_\mu\psi)\partial^\nu(\bar{\psi}\gamma^\mu\psi) \\
& -\frac{1}{2}\delta_{TS}\partial_\nu(\bar{\psi}\vec{\tau}\psi)\partial^\mu(\bar{\psi}\vec{\tau}\psi) \\
& -\frac{1}{2}\delta_{TV}\partial_\nu(\bar{\psi}\vec{\tau}\gamma_\mu\psi)\partial^\nu(\bar{\psi}\vec{\tau}\gamma^\mu\psi) \\
& -\frac{1}{4}F^{\mu\nu}F_{\mu\nu} - e\frac{1-\tau_3}{2}\bar{\psi}\gamma^\mu\psi A_\mu .
\end{aligned}
$$

Zhao, Li, Yao, and Meng, PRC **82**, 054319 (2010)

$$\sigma = \sqrt{\frac{\sum_{i=1}^{N}(M^i_{\rm exp} - M^i_{\rm theo})^2}{N}} \quad ({\rm MeV})$$

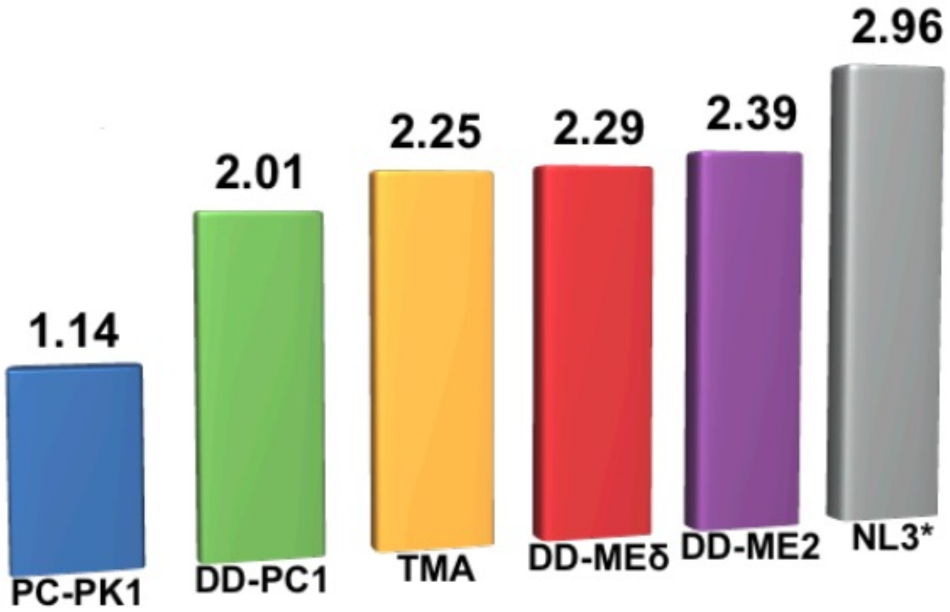

S.E. Agbemava, *et al.* PRC **89**, 054320 (2014)
L. S. Geng, *et al.* PTP **113**, 785 (2005)

Best density functional description for nuclear masses so far.

Optical potential in relativistic framework

- Schrödinger-like equation for the upper component of the Dirac spinor

$$\left[-\frac{\nabla^2}{2E} + V_{\mathrm{cent}}(r) + V_{\mathrm{so}}(r)\boldsymbol{\sigma}\cdot\boldsymbol{l} + V_{\mathrm{Darwin}}(r)\right]\phi(\boldsymbol{r}) = \frac{E^2 - M^2}{2E}\phi(\boldsymbol{r})$$

✓ Components of the optical potential

$$V_{\mathrm{cent}}(r) = \frac{M}{E}U_S + U_0 + \frac{1}{2E}(U_S^2 - U_0^2)$$

$$V_{\mathrm{so}}(r) = -\frac{1}{2rE}\left(\frac{D'}{D}\right)$$

$$V_{\mathrm{Darwin}}(r) = \frac{3}{8E}\left(\frac{D'}{D}\right)^2 - \frac{1}{2rE}\left(\frac{D'}{D}\right) - \frac{1}{4E}\left(\frac{D''}{D}\right)$$

$$D = M + U_S + E - U_0$$

→ Differential cross section $d\sigma/d\Omega$, analyzing power A_y, spin rotation function Q

Low-density extrapolation $\rho \leq 0.08\ \mathrm{fm}^{-3}$ for U_S, U_0

- CTOM: values for U_S, U_0 at $\rho = 0.04, 0.06\ \mathrm{fm}^{-3}$ are adjusted to n, p + 40Ca, ^{208}Pb
- In this work: $U_i = a_i\rho^2 + b_i\rho + c_i \rightarrow U_i|_{0.08}, U_i'|_{0.08}$, and $U_i|_0 = 0$, with $i = S, 0$

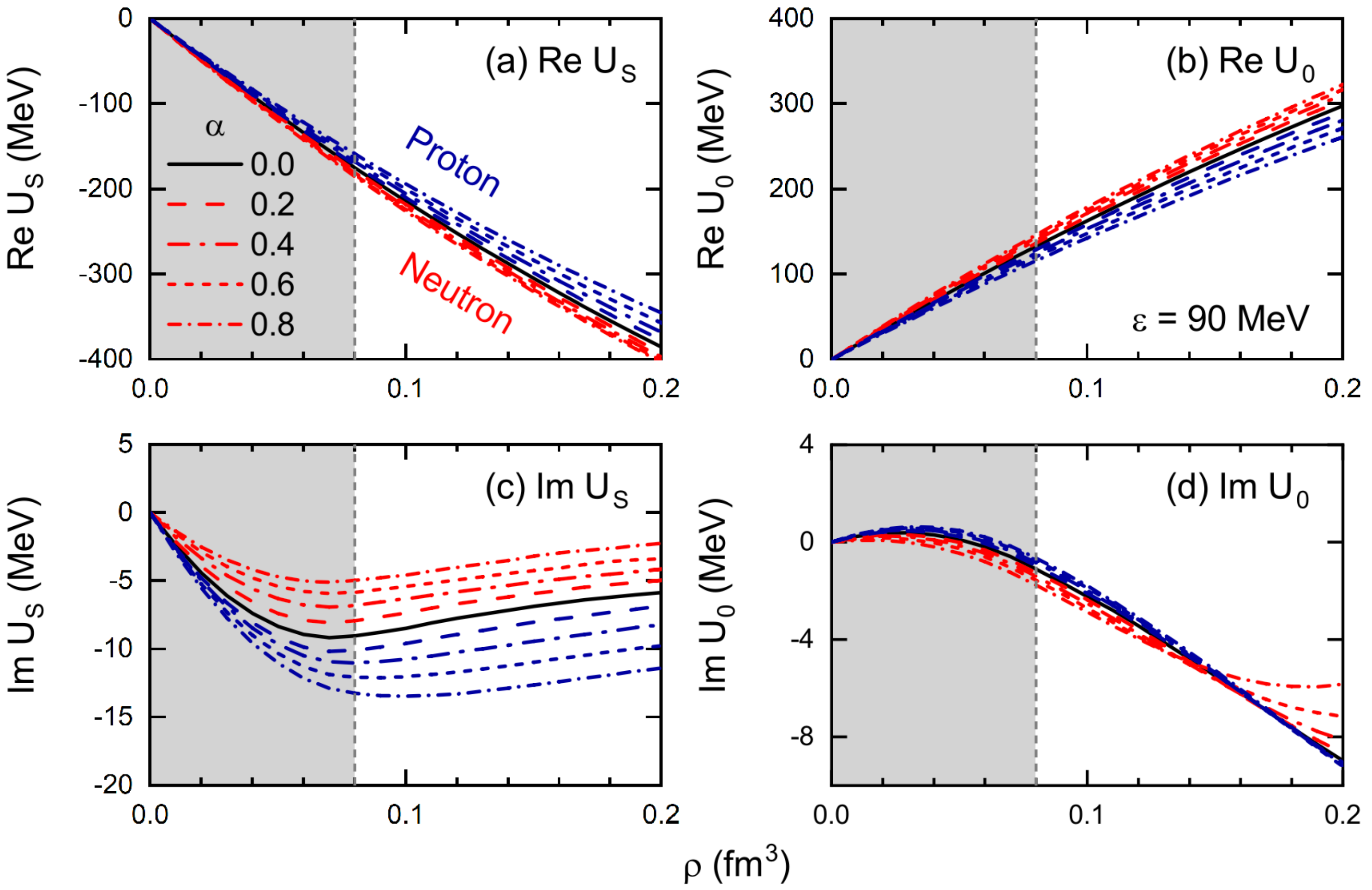

Contents

Central term: comparison with GOP and CTOM

- Central terms of RBOM potential in comparison with GOP and CTOM

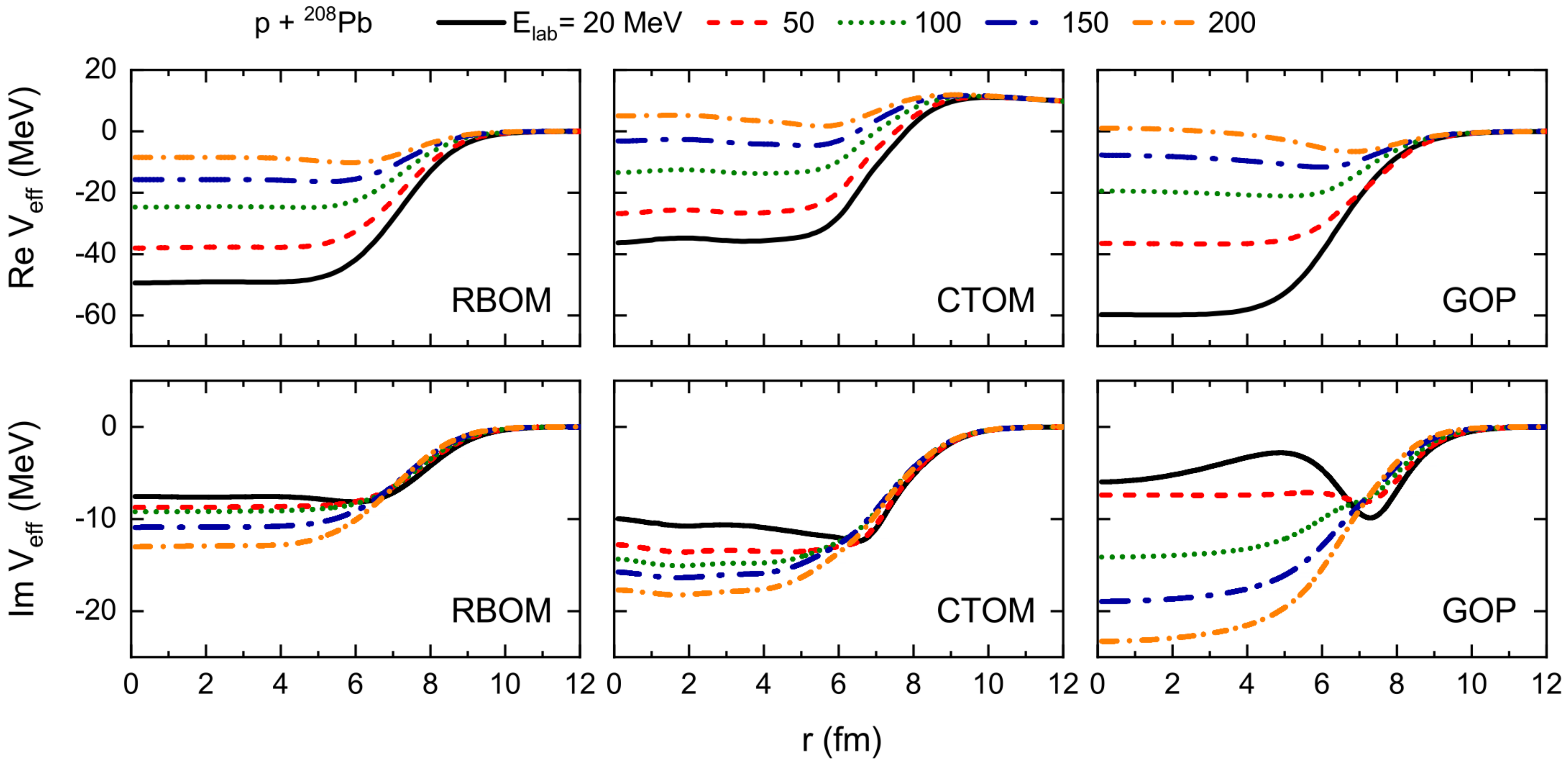

GOP: PRC **80**, 034605 (2009), CTOM (RBHF-projection + ILDA): PRC **94**, 034606 (2016)

Spin-orbit term: comparison with GOP and CTOM

- Spin-orbit terms of RBOM potential in comparison with GOP and CTOM

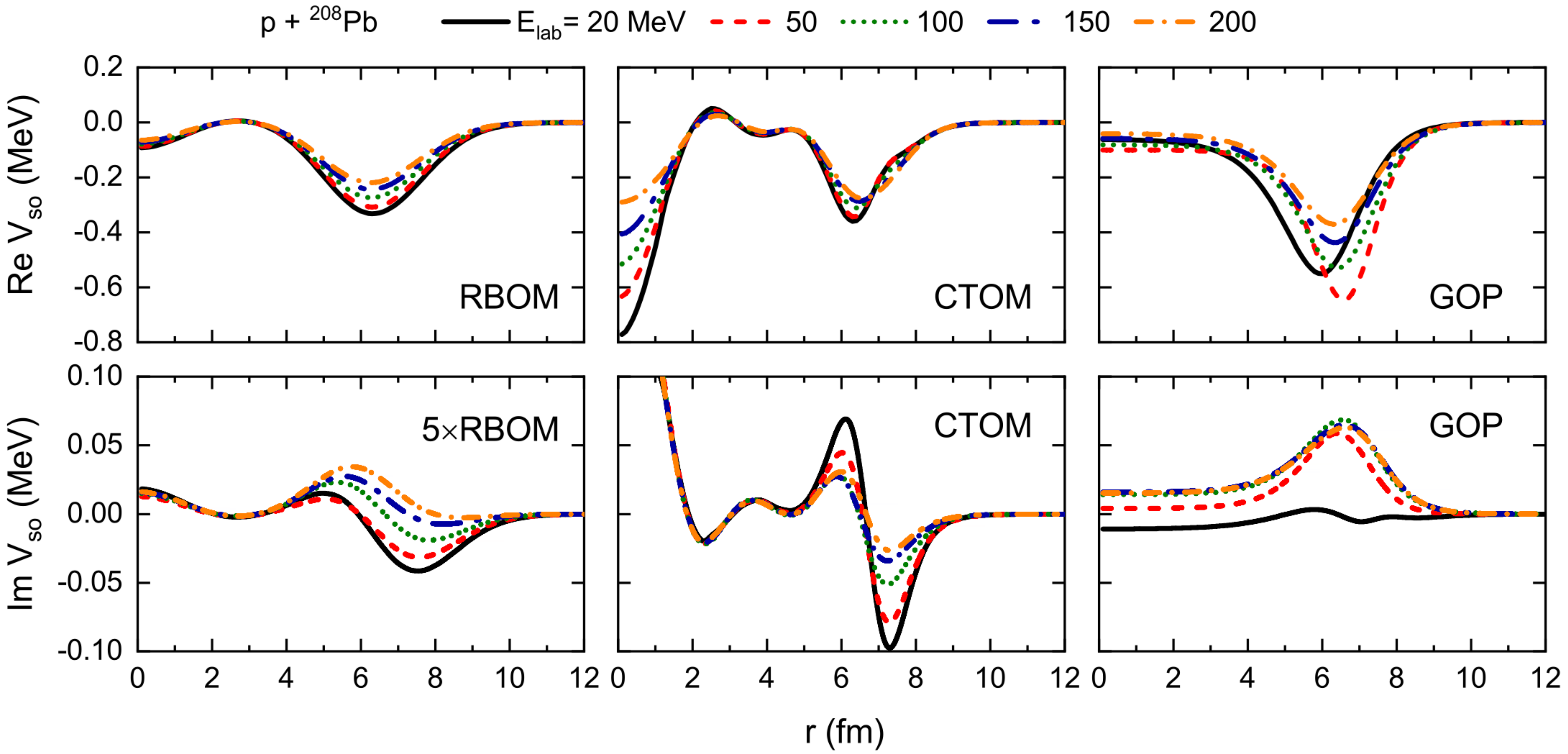

RBOM: Relativistic Mean Field with PC-PK1, CTOM: Hartree-Fock Bogoliubov with Gogny D1S

Differential cross section: $p + {}^{208}\text{Pb}$

- Differential cross section $d\sigma/d\Omega$ in comparison with experimental data and GOP

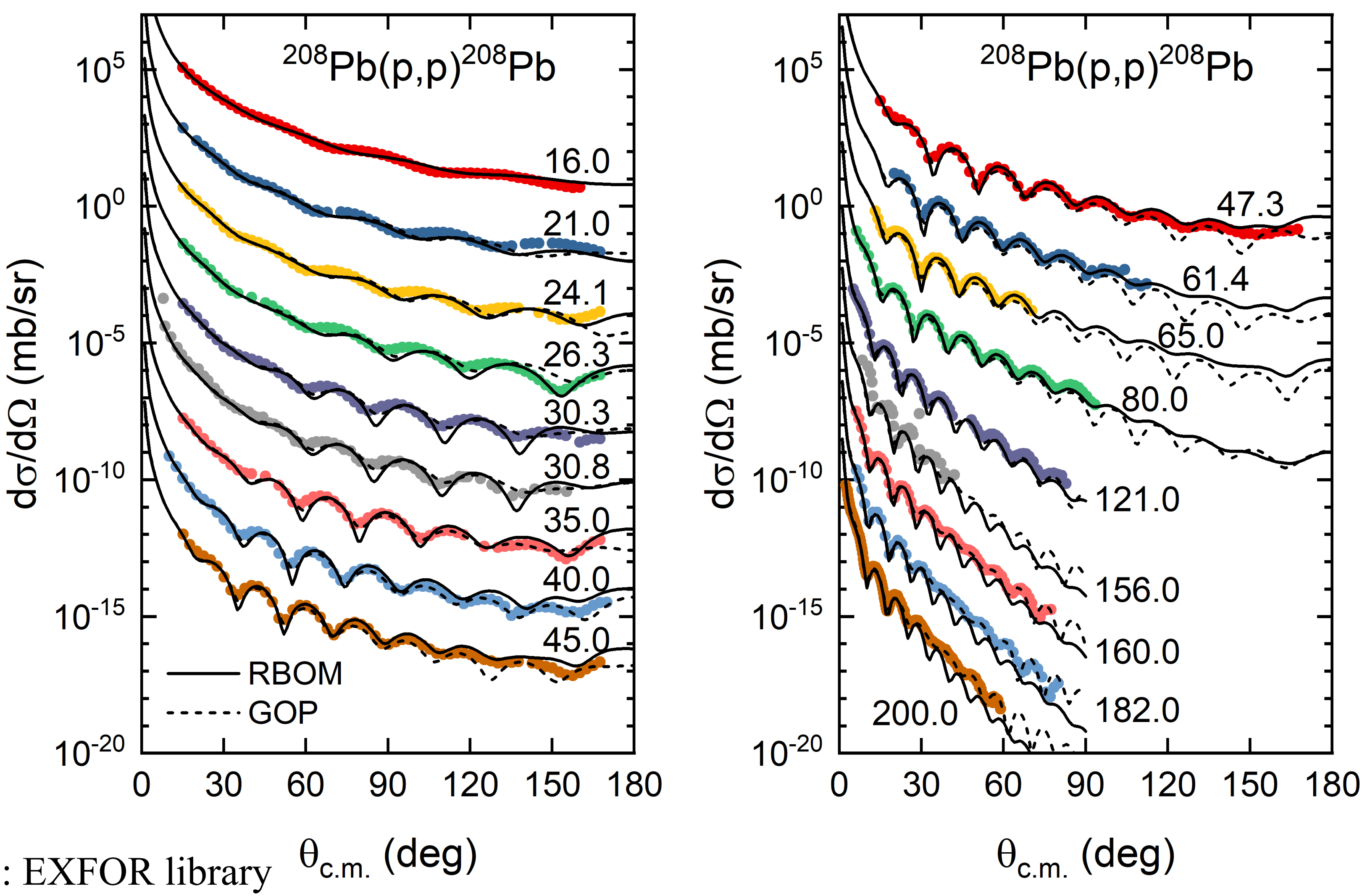

True vales

$\times 10^{-2}$

$\times 10^{-4}$

…

Exp. data.: EXFOR library

Differential cross section: $p + {}^{120}\text{Sn}$

- Differential cross section $d\sigma/d\Omega$ in comparison with experimental data and GOP

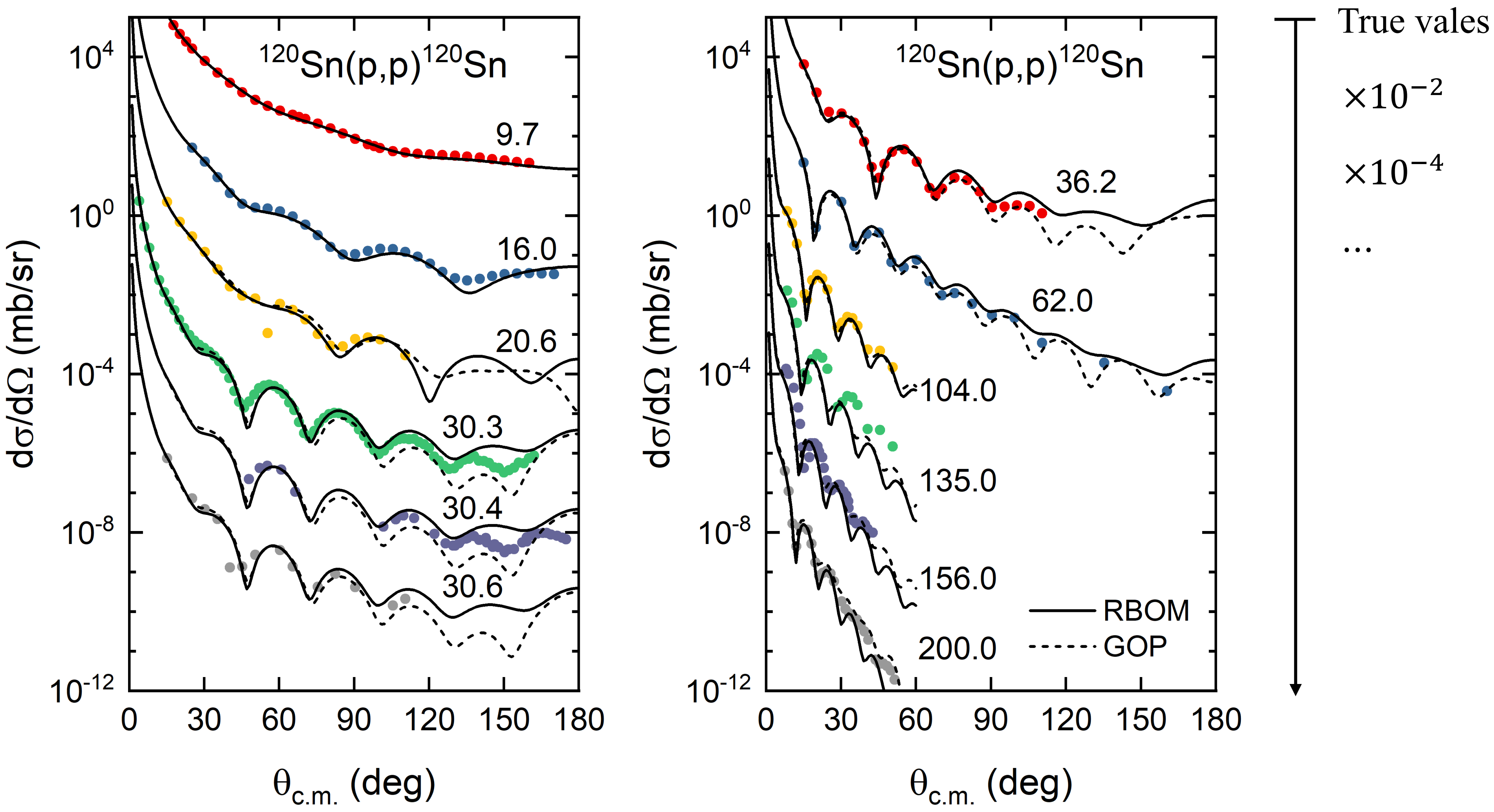

Differential cross section: $p + {}^{90}Zr$

- Differential cross section $d\sigma/d\Omega$ in comparison with experimental data and GOP

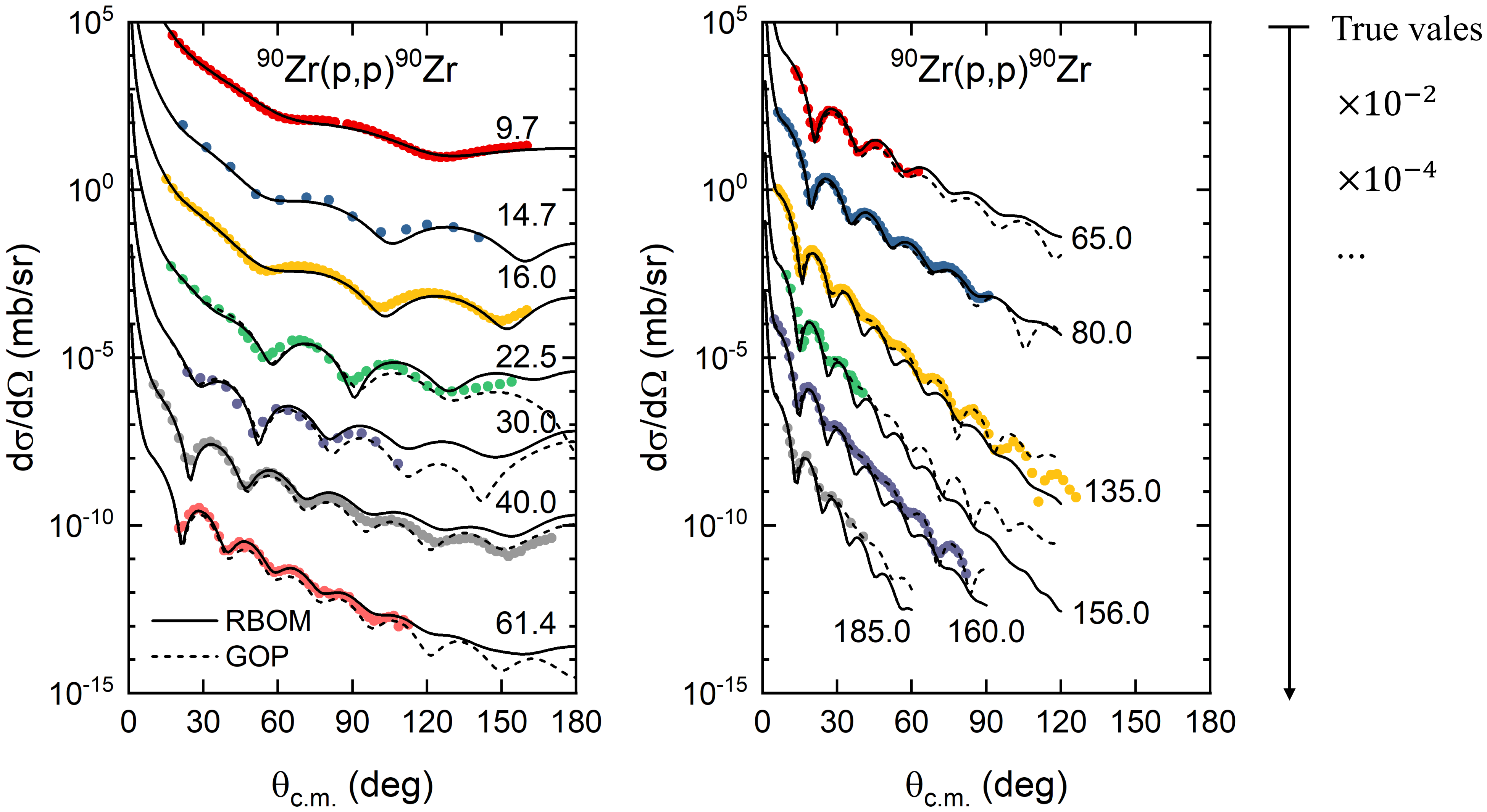

Differential cross section: p + ^{48}Ca

- Differential cross section $d\sigma/d\Omega$ in comparison with experimental data and GOP

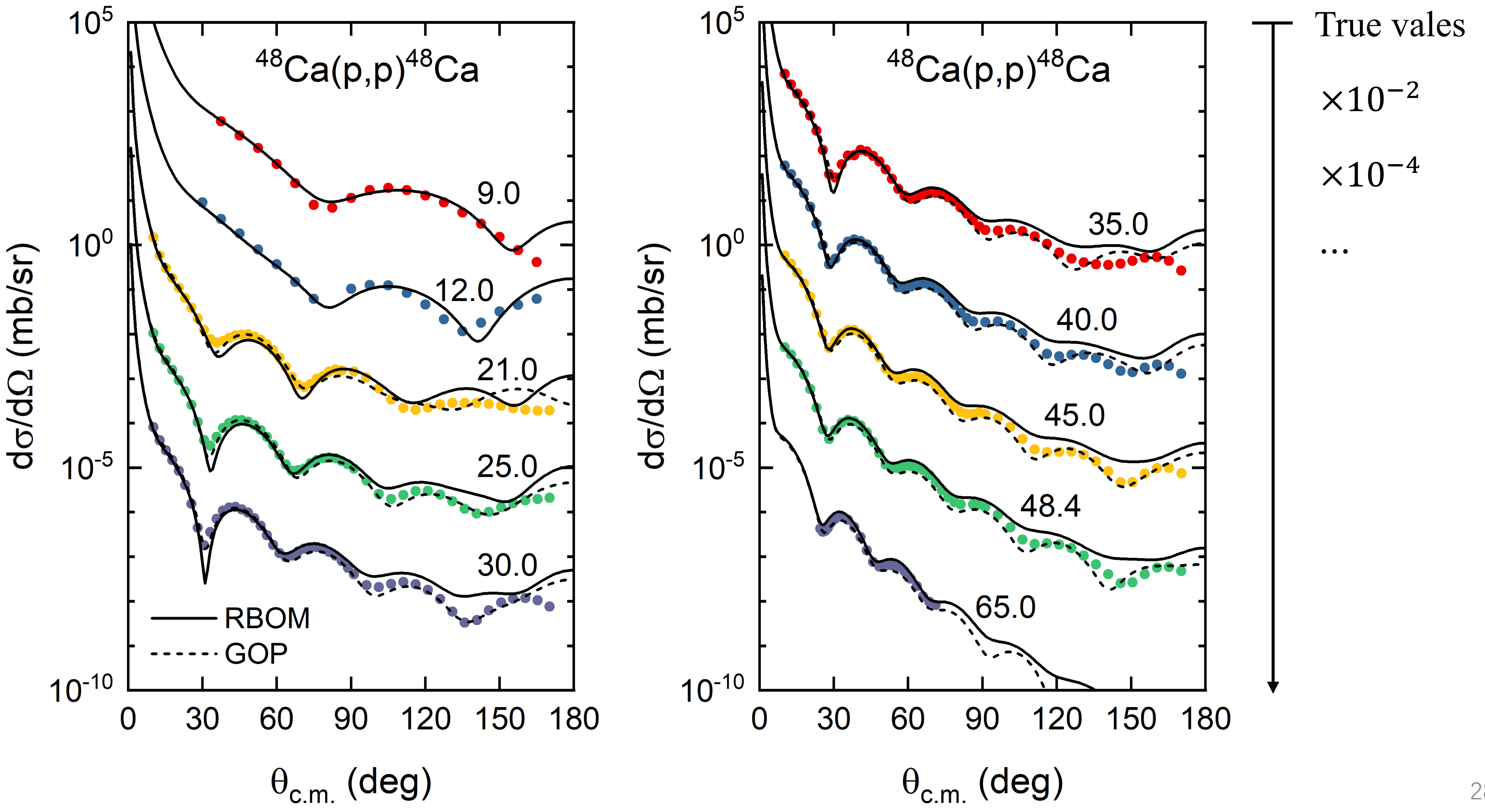

Differential cross section: $p + {}^{40}\mathrm{Ca}$

- Differential cross section $d\sigma/d\Omega$ in comparison with experimental data and GOP

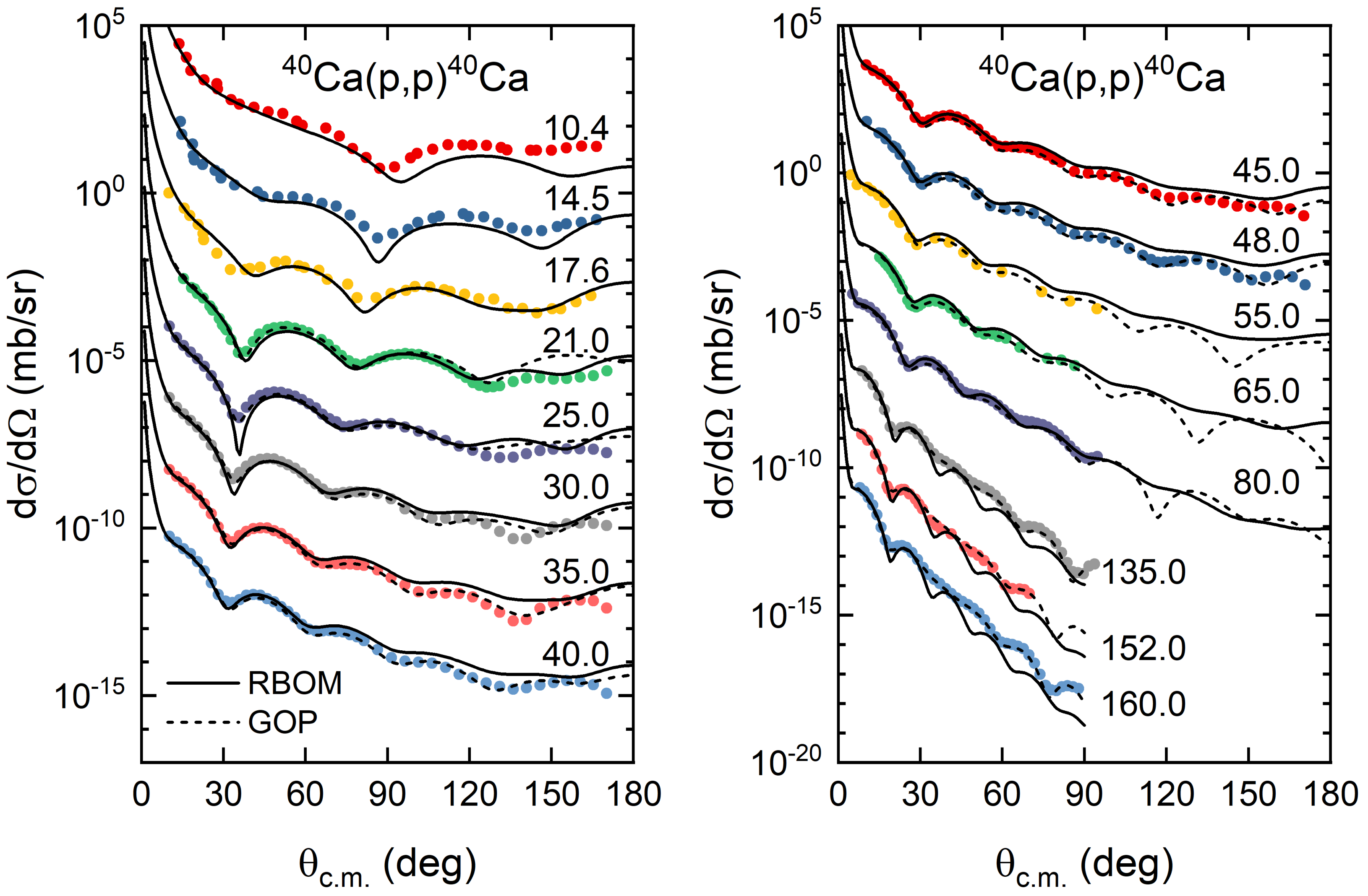

True vales

$\times 10^{-2}$

$\times 10^{-4}$

…

Differential cross section: $n + {}^{208}Pb$

- Differential cross section $d\sigma/d\Omega$ in comparison with experimental data and KD03

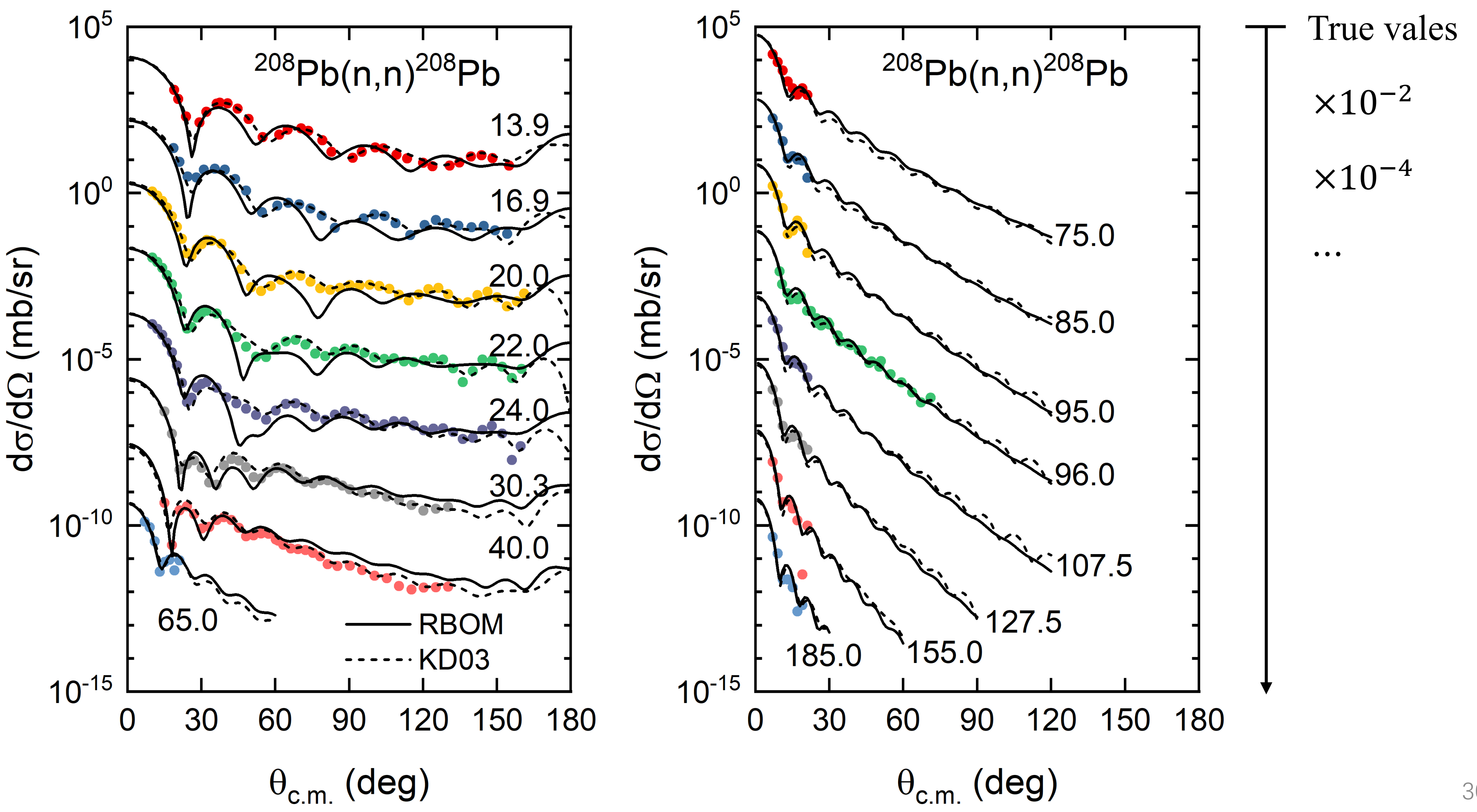

Spin observables: p + ^{208}Pb

- Analyzing power A_y and spin rotation function Q from RBOM potential

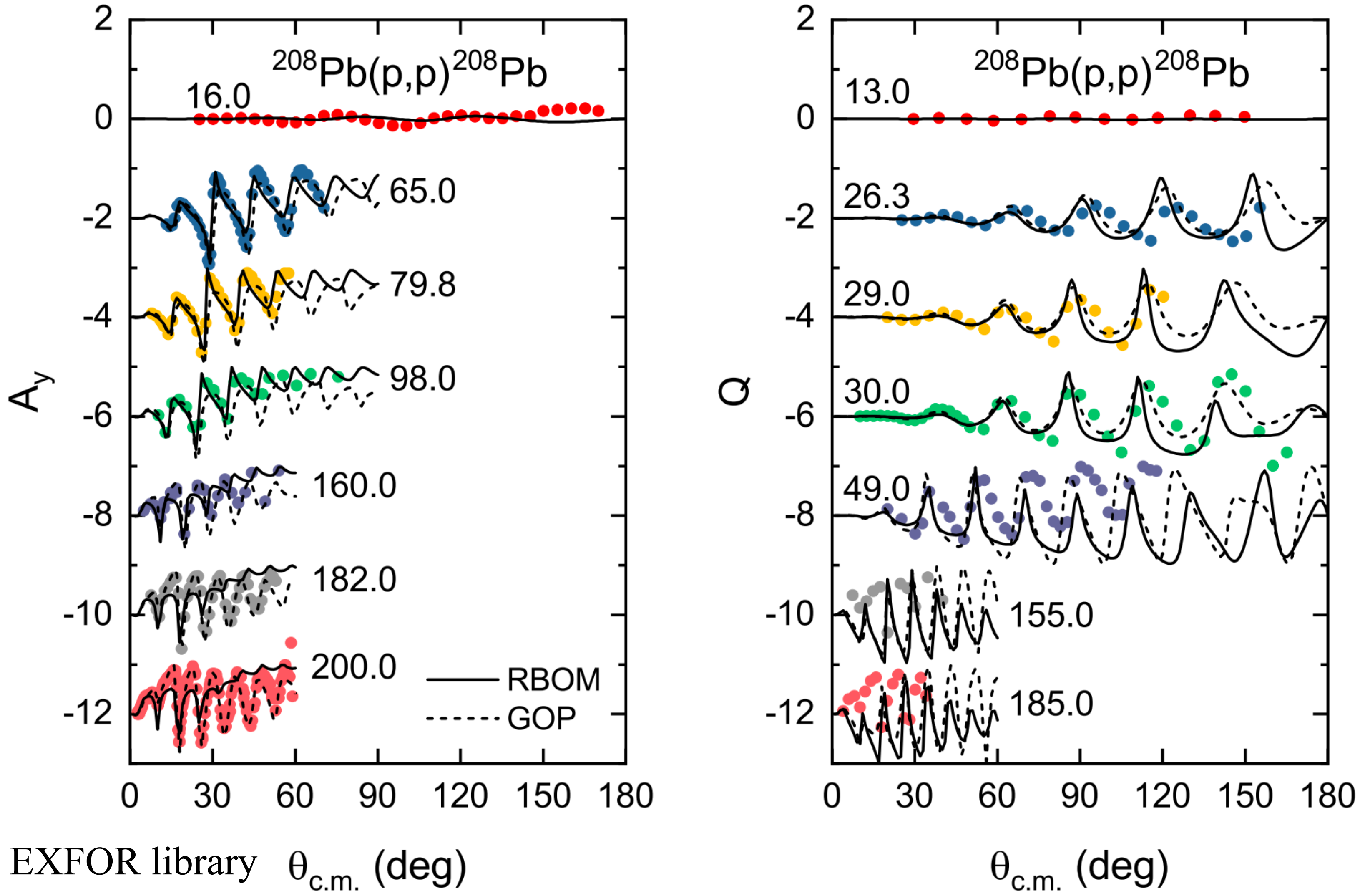

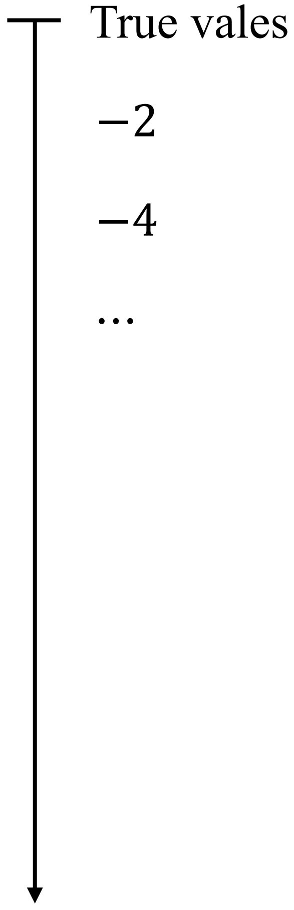

Exp. data.: EXFOR library

Uncertainty analysis for RBOM

- Uncertainties for RBOM (RBHF + ILDA) have two sources:
  - *Effective range parameter* t in ILDA: $1.25 \leq t \leq 1.35$ fm
  - *Realistic NN interactions*: Bonn A, B, C

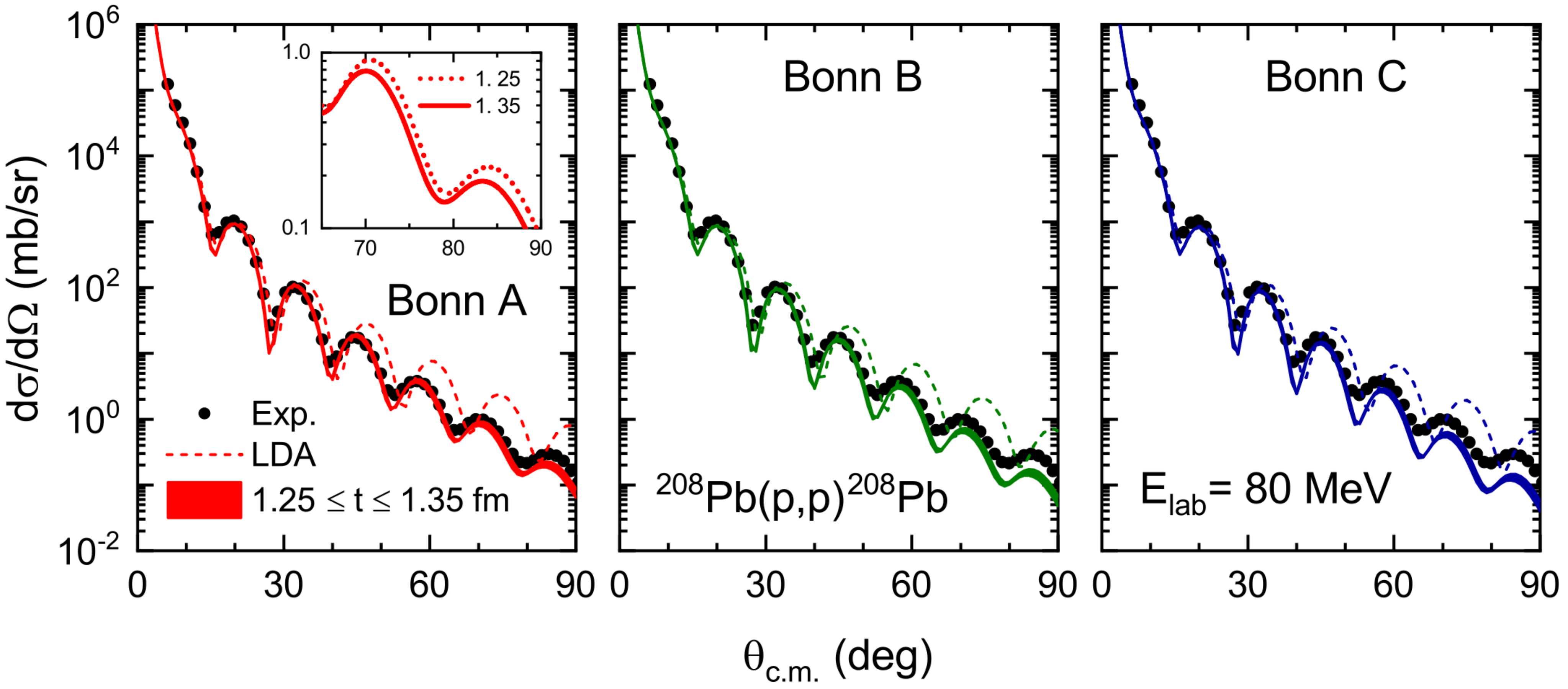

Performance of RBOM at high incident energies

- The underestimation of cross section angular distributions at high energies is related to the large momentum dependence of single-particle potentials in nuclear matter

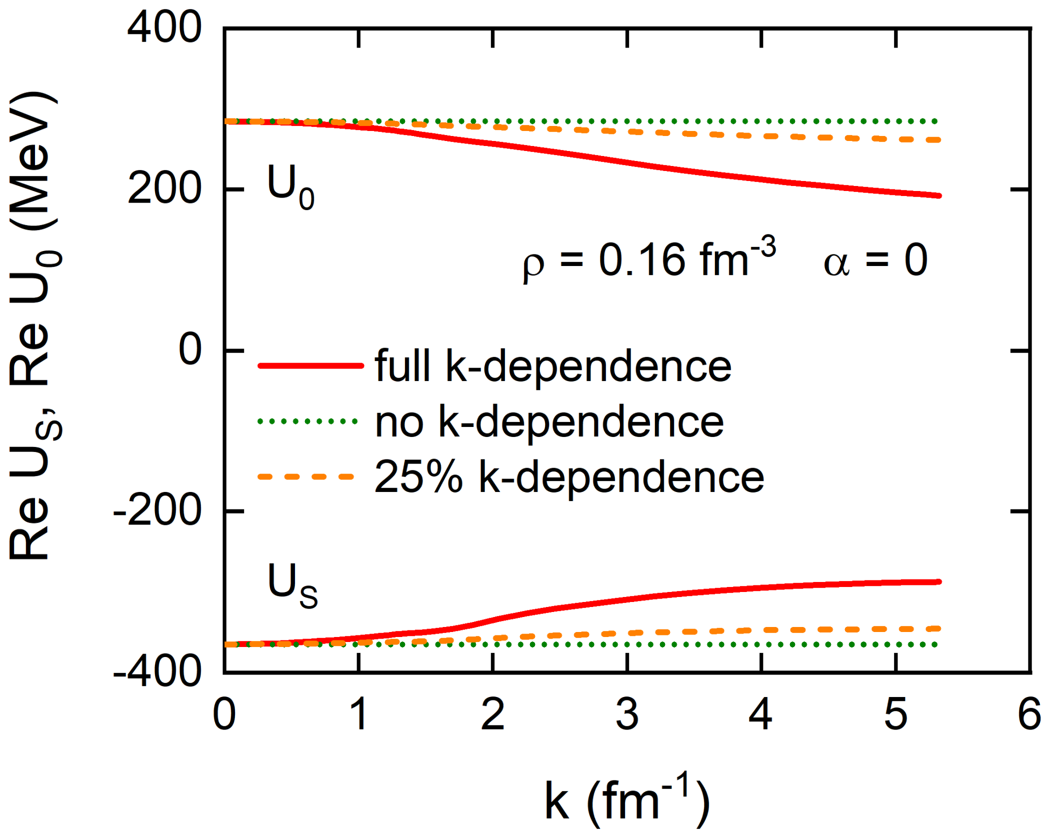

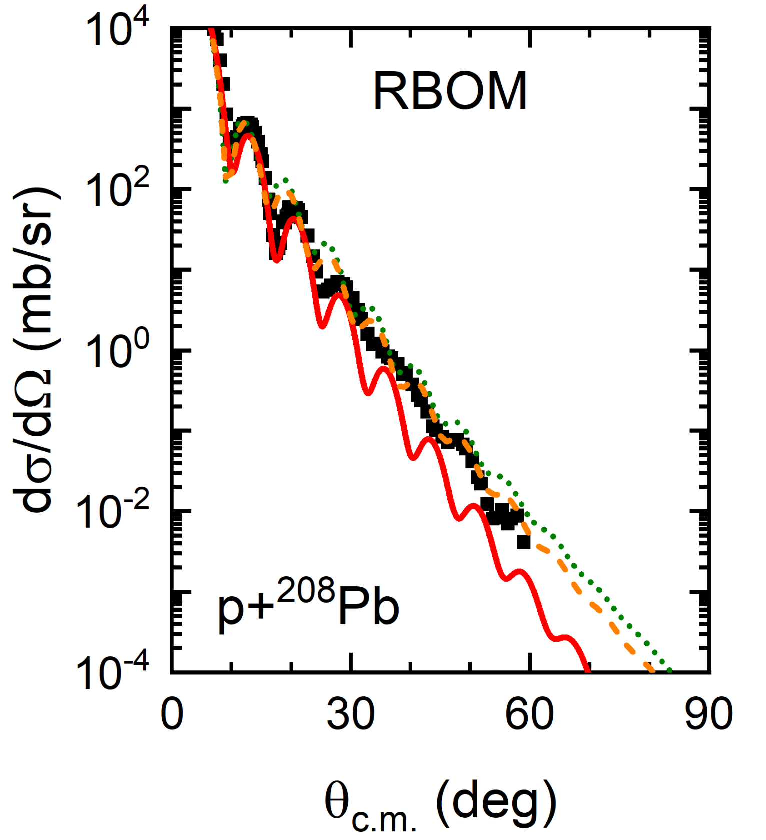

→ Weaker momentum dependence, better angular distributions

Cross sections: $p/n + {}^{208}\text{Pb}$

- Proton reaction cross sections and neutron total cross sections from RBOM

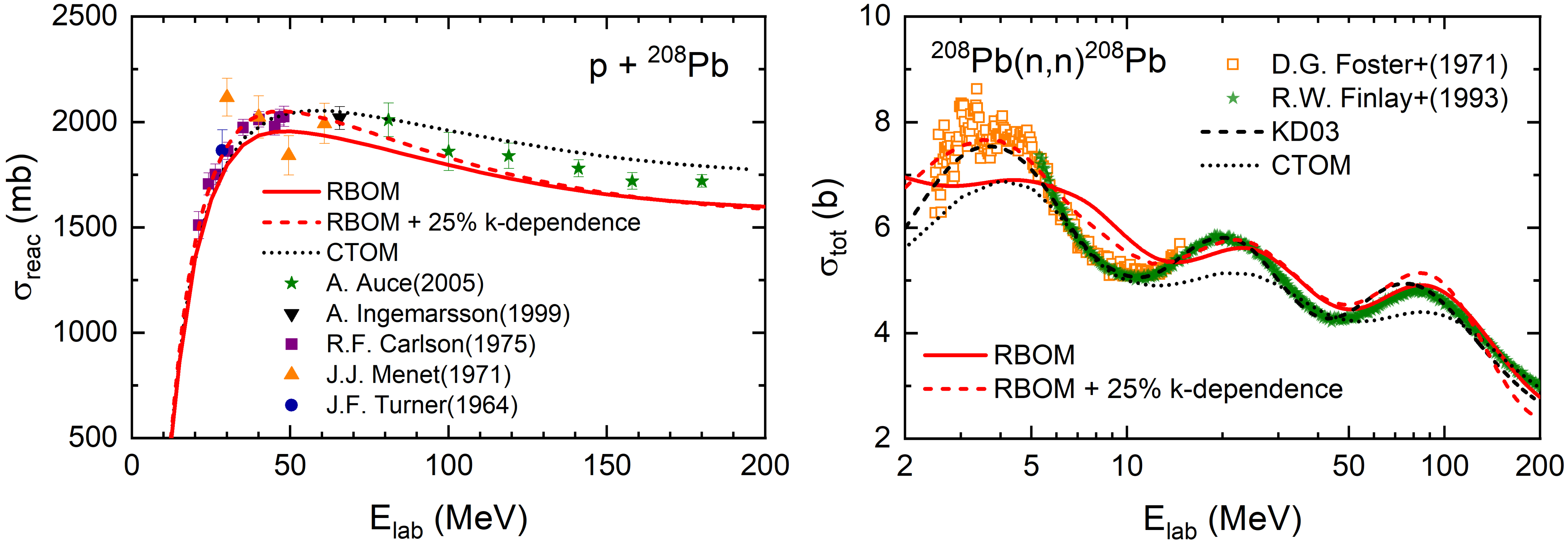

✓ Overall, cross sections from RBOM are close to experimental data

✓ Weaker momentum dependence improves neutron results at low energies

Fully self-consistent RBHF calculation for finite nuclei

$$\langle ab|\bar{G}(W)|a'b'\rangle = \langle ab|\bar{V}|a'b'\rangle + \frac{1}{2}\sum_{cd}\langle ab|\bar{V}|cd\rangle \frac{Q}{W-\varepsilon_c-\varepsilon_d}\langle cd|\bar{G}(W)|a'b'\rangle$$

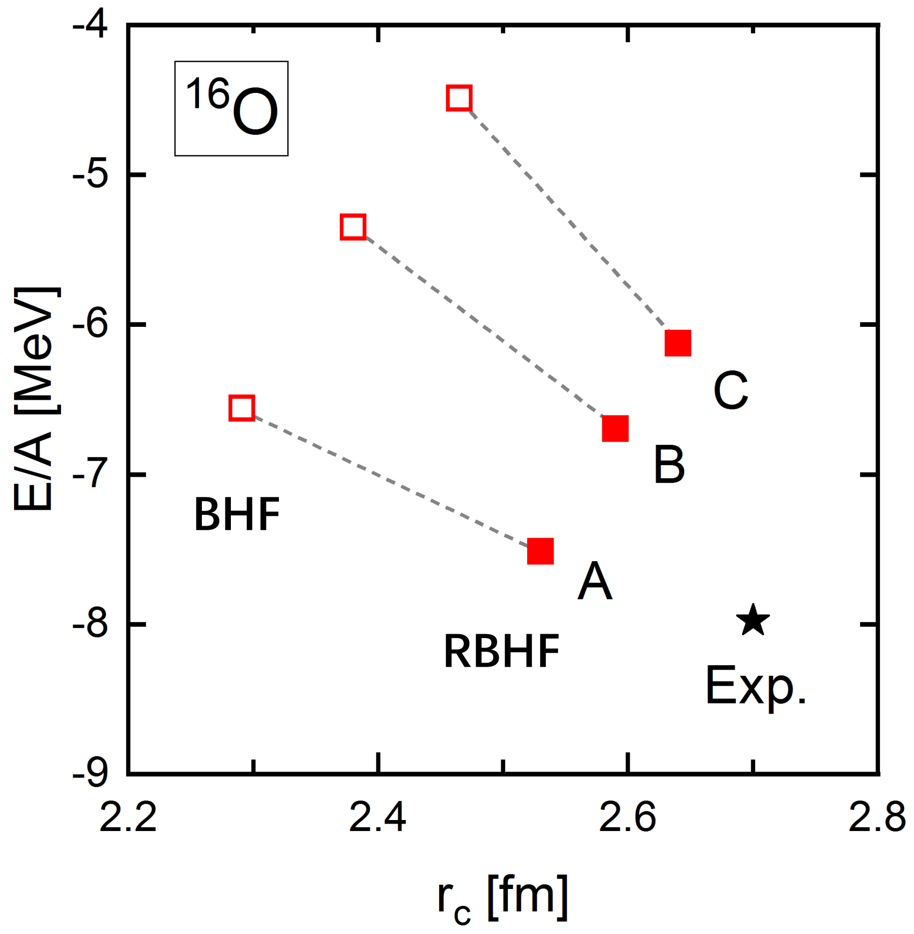

Shen, Liang, Meng, Ring, and Zhang, PRC **96**, 014316 (2017)
Shen, Liang, Long, Meng, and Ring, PPNP **109**, 103713 (2019)

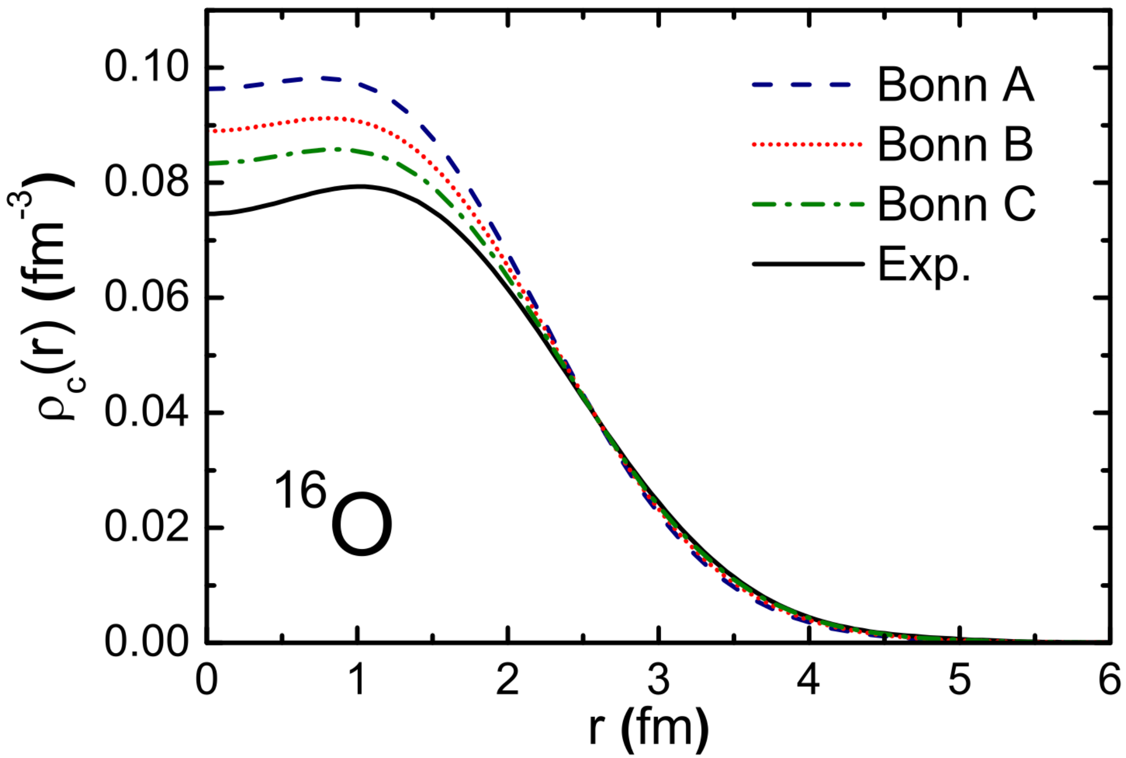

Towards consistent nuclear structure and reactions

- Angular distribution from RBOM with **self-consistent densities**

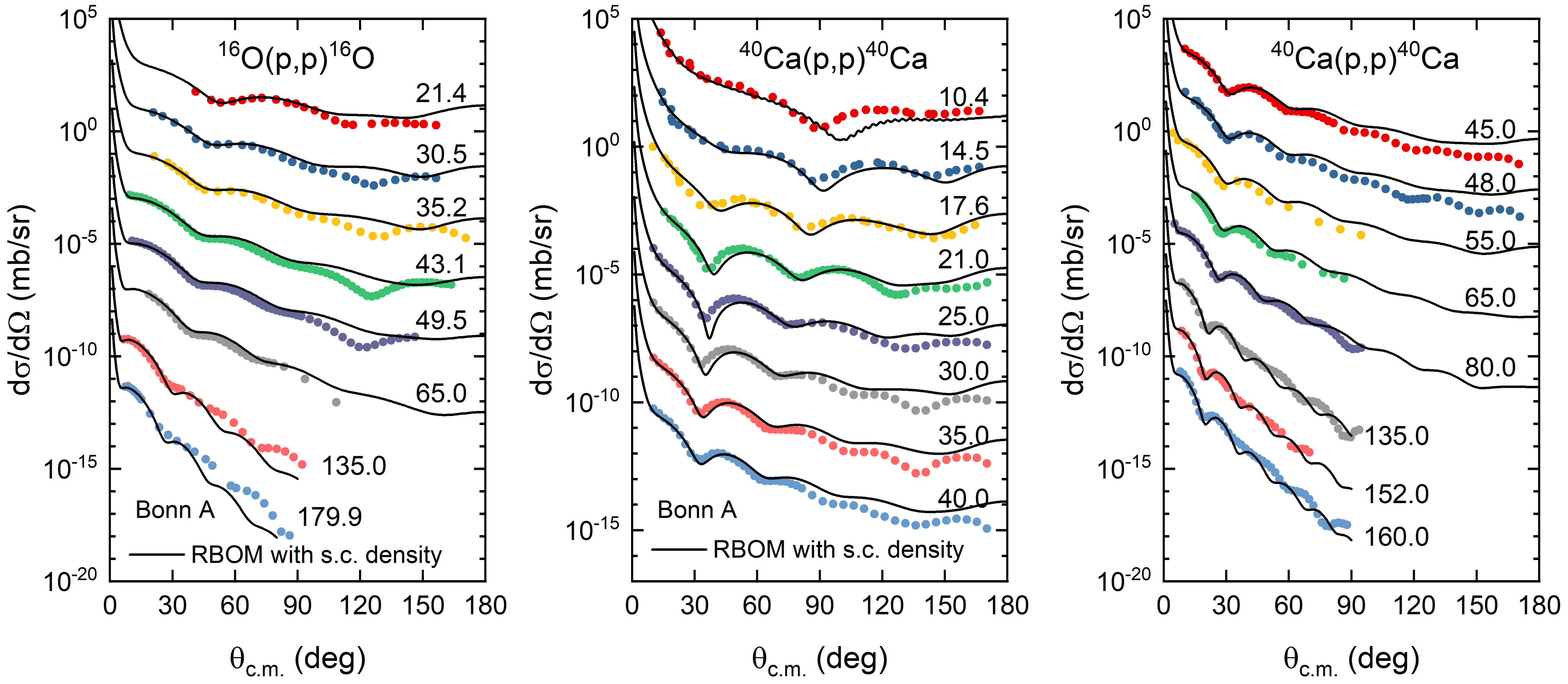

Summary

- We have developed a microscopic **RBOM** potential
  - ✓ Relativistic BHF with local density approximation
  - ✓ No ambiguities for single-particle potentials
  - ✓ No free parameter other than effective range t
- Satisfactory description for differential cross section, spin observables for p/n + spherical nuclei
- We anticipate **RBOM** potential could provide:
  - ✓ reference for other optical potentials
  - ✓ reliable description for exotic nuclei

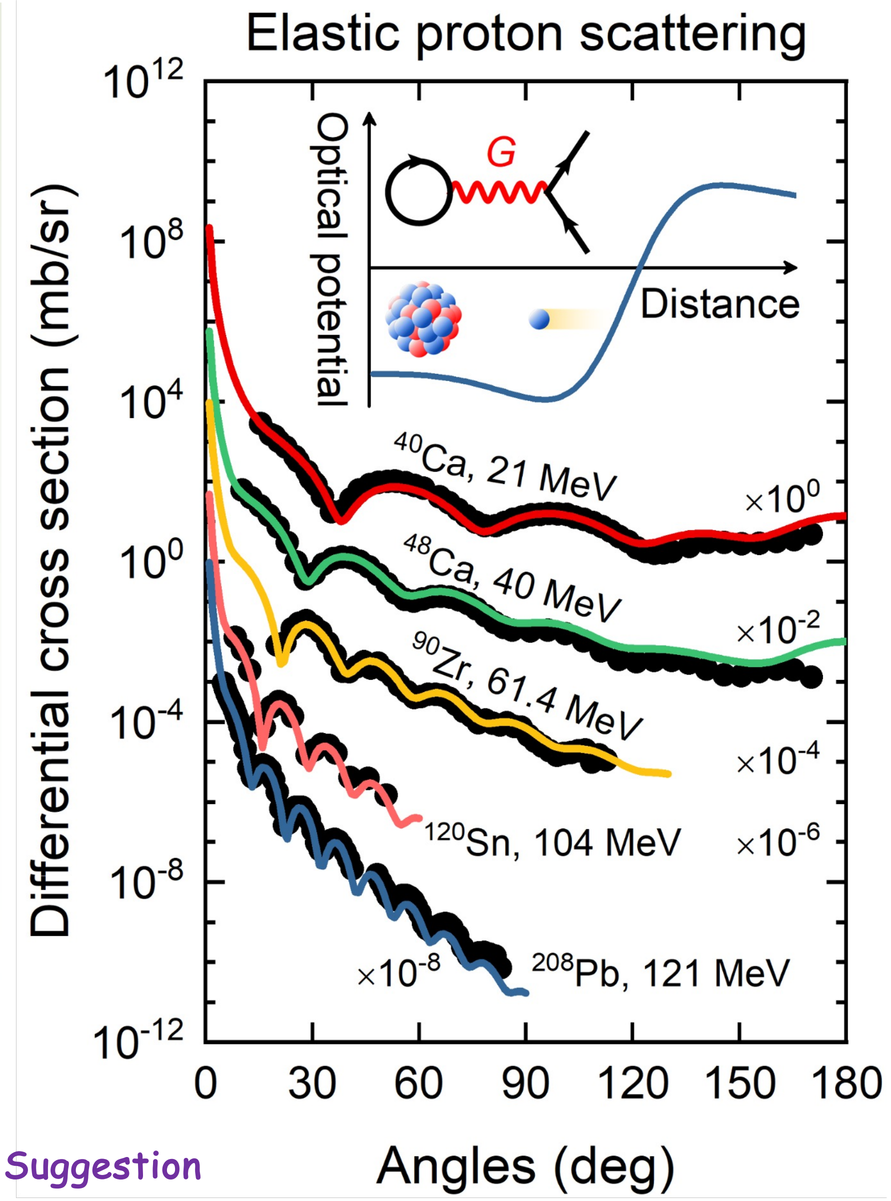

Qin, Wang*, Tong, Zhao, Wang, Li, and Ring, PRC **109**, 064603 (2024), **Editor's Suggestion**